Efficient biosynthetic incorporation of tryptophan analogues, and spectroscopic characterization of tryptophan-analogue labelled LysM proteins

Petrovic, Dejan

Efficient biosynthetic incorporation of tryptophan analogues, and spectroscopic characterization of tryptophan-analogue labelled LysM proteins

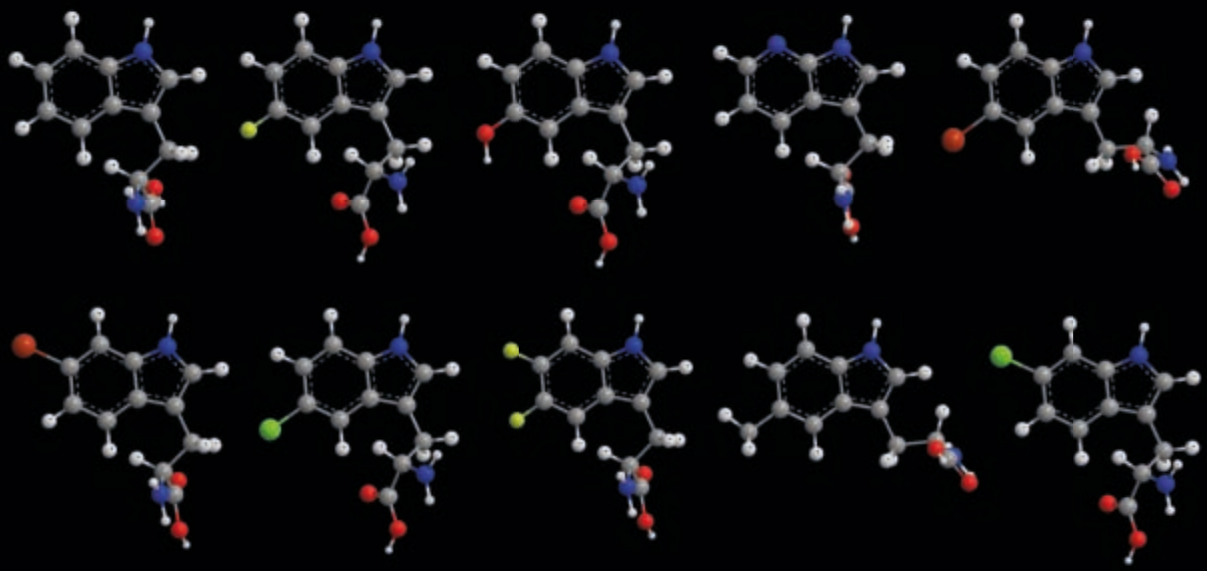

Dejan Petrović

Efficient biosynthetic incorporation of tryptophan analogues, and spectroscopic characterization of tryptophan-analogue labelled LysM proteins

Dejan Petrović

Dejan Petrović
Efficient biosynthetic incorporation of tryptophan analogues, and spectroscopic characterization of tryptophan-analogue labelled LysM proteins
PhD thesis, Groningen Biomolecular Sciences and Biotechnology Institute,
University of Groningen, the Netherlands

First published 2013

Published in the Netherlands
by University of Groningen, Groningen

Printed in Groningen
by NetzoDruk

Typset from a TEX/LATEX file prepared by Vibor Jelić and the author
Cover design by Marija Radišić

ISBN 978-90-367-6737-8
ISBN 978-90-367-6736-1 (electronic version)

rijksuniversiteit
groningen

Efficient biosynthetic incorporation of tryptophan analogues, and spectroscopic characterization of tryptophan-analogue labelled LysM proteins

Proefschrift

ter verkrijging van de graad van doctor aan de
Rijksuniversiteit Groningen
op gezag van de
rector magnificus, prof. dr. E. Sterken
en volgens besluit van het College voor Promoties.

De openbare verdediging zal plaatsvinden op

vrijdag 7 februari 2014 om 16.15 uur

door

Dejan Petrović

geboren op 17 november 1982

te Karlovac, Kroatië

Promotor:

Prof. dr. B.W. Dijkstra

Copromotor:

Dr. J. Broos

Beoordelingscommissie:

Prof. dr. E.J. Boekema
Prof. dr. J. Kok
Prof. dr. G.T. Robillard

"The sun is the same in a relative way but you're older,
shorter of breath and one day closer to death."
Pink Floyd, *Time*

Contents

Chapter 1

Introduction

1.1 Fluorescence

1.1.1 Phenomenon of fluorescence and phosphorescence

Phenomena now known as fluorescence and phosphorescence were mentioned in Chinese books as far back as 1500 BC, but analysing, controlling and using these phenomena started only 150 years ago. Fluorescence as a research topic was brought to light by Sir George Gabriel Stokes. In 1852, he described the luminescence observed in the fluorspar mineral (calcium fluoride) as fluorescence [1].

Today we know that fluorescence is just one type of luminescence. More specifically, luminescence (Latin word lumen = light) is the ability of substances to emit light when illuminated by a light source. Photon absorption can promote an electron from the S_0 ground level to a vibrational level of the first electronic state (S_1), or higher electronic state (S_n, where $n \geq 2$). In the time-range of 10^{-12} seconds or less electrons return to the lowest vibrational level of S_1. This process is called internal conversion (IC). Return of the electron to S_0 can result in two types of luminescence: fluorescence or phosphorescence. When the electron returns from S_1 to S_0 we speak of fluorescence emission. Substances which are able to emit fluorescence are known as fluorophores. For small organic molecules fluorescence typically occurs in the time-range of 10^{-8} seconds. Phosphorescence occurs when the electron in the first electronic excited state (S_1), instead of returning to the S_0, undergoes a spin conversion to the first triplet state, T_1. This process from S_1 to T_1, is called intersystem crossing (ISC) and occurs at a similar time range as fluorescence. The electron in T_1 has the same spin orientation as the electron in the S_0 orbital from which it originated. Return of the electron from T_1 to S_0 is very slow as this is a so called forbidden transition. Phosphorescence typically occurs in the time-range of milliseconds to seconds. The processes that occur upon the absorption of a photon can be presented schematically in a Jabloński diagram [2] (Figure 1.1).

1.1.2 Quantum yield and fluorescence lifetime

Two important characteristics of a fluorophore are its fluorescence lifetime (τ) and its quantum yield (Q). The fluorescence lifetime is the average time the fluorophore spends in the excited state. The fluorescence lifetime is equal to the reciprocal of the sum of all depopulation rates from S_1 to S_0 (equation 1a).

$$\tau = \frac{1}{\Gamma + \sum k_{nr}} \quad \text{(1a)}$$

Γ - emission rate of the fluorophore
$\sum k_{nr}$ - sum of all non-radiative decay processes

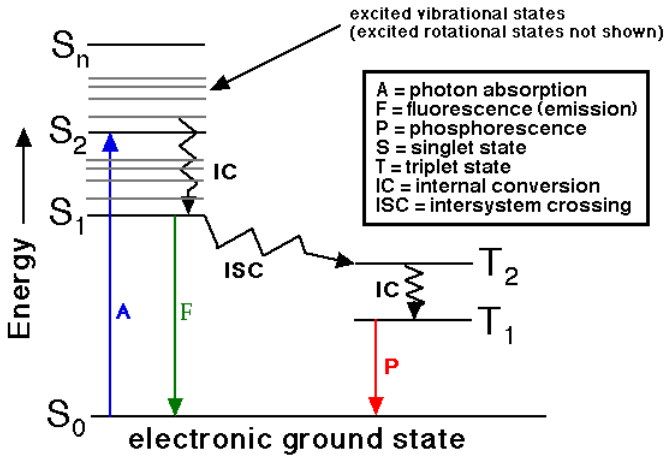

Figure 1.1: Jablonski diagram

The lifetime of the uorophore in the absence of non-radiative processes is called the intrinsic or natural lifetime, χ_n (equation 1b).

$$\chi_n = \frac{1}{} \quad \text{(1b)}$$

χ_n is a property of the molecule and is usually not sensitive to the uorophore microenvironment while the magnitude of k_{nr} is dependent on the microenvironment. The uorescence quantum yield (Q) is the ratio of the number of emitted photons to the number of absorbed photons (equation 1c), and can be expressed as a function of and k_{nr} as follows:

$$Q = \frac{}{+ k_{nr}} \text{ or } Q = \frac{\chi}{\chi_n} \quad \text{(1c)}$$

The quantum yield ranges from 0 1. If k_{nr} then Q approaches 0. In the ideal case when $k_{nr} = 0$ all absorbed photons are emitted as uorescence, and Q = 1. Because the value of Q is always changing with k_{nr}, a change of the uorophore s microenvironment often results in a measurable change in the quantum yield.

1.1.3 Quenching of uorescence

The process resulting in a decrease of the uorescence intensity of a uorophore is known as quenching. Fluorescence quenching can be caused by many di erent molecular processes such as excited-state reactions, radiationless energy transfer, or complex formation with a quencher [3]. Collisional or dynamic quenching is a process in which the

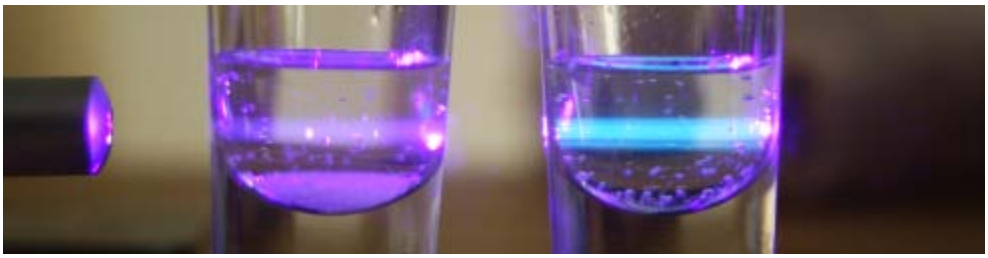

Figure 1.2: Quinone quenching with potassium iodide. Left: Quinone solution with potassium iodide, Right: Quinone solution without potassium iodide

fluorophore in the excited state collides with a quencher. This collision results in radiationless de-excitation of the fluorophore. In the case of static quenching, a non-fluorescent complex between fluorophore and quencher is formed. Many compounds are known as quenchers of fluorescence. For small aromatic fluorophores, like indole, good quenchers are iodide, amines and electron deficient molecules like acrylamide. The potential of a collisional quencher to suppress fluorescence of a certain fluorophore can be investigated in a Stern-Volmer (S-V) quenching experiment. The extent of quenching at different quencher concentrations is recorded and analysed using the S-V equation:

$$\frac{F_0}{F} = 1 + k_q \tau_0 [Q] = 1 + K_{SV}[Q] \quad \text{(4a)}$$

F_0 - The emission intensity in the absence of quencher.
F - The emission intensity in the presence of quencher.
k_q $[M^{-1}s^{-1}]$ - The collisional quenching constant.
τ_0 [s] - The lifetime of the fluorophore in the absence of quencher.
K_{SV} $[M^{-1}]$ - Stern-Volmer constant (quencher concentration at which 50% of the intensity is quenched.
[Q]- The concentration of a quencher.

When a linear S-V plot, $\frac{F_0}{F}$ versus [Q], is obtained all fluorophores are equally accessible to the quencher. If the S-V plot shows a downward curvature the solvent accessibility is not equal for all fluorophores in the sample. An upward curvature is observed if both a dynamic and a static quenching mechanism are operative. Collisional quenching experiments are widely used for determining the solvent accessibility of tryptophan in a protein [4, 5, 6, 7, 8] (Figure 1.3). If the tryptophan is buried inside the protein, quenching is not expected to be very efficient, yielding a low k_q and K_{SV} value. If the tryptophan residue is on the protein surface then efficient quenching is expected, with a k_q value approaching the diffusional rate constant of the quencher. Proteins usually contain several

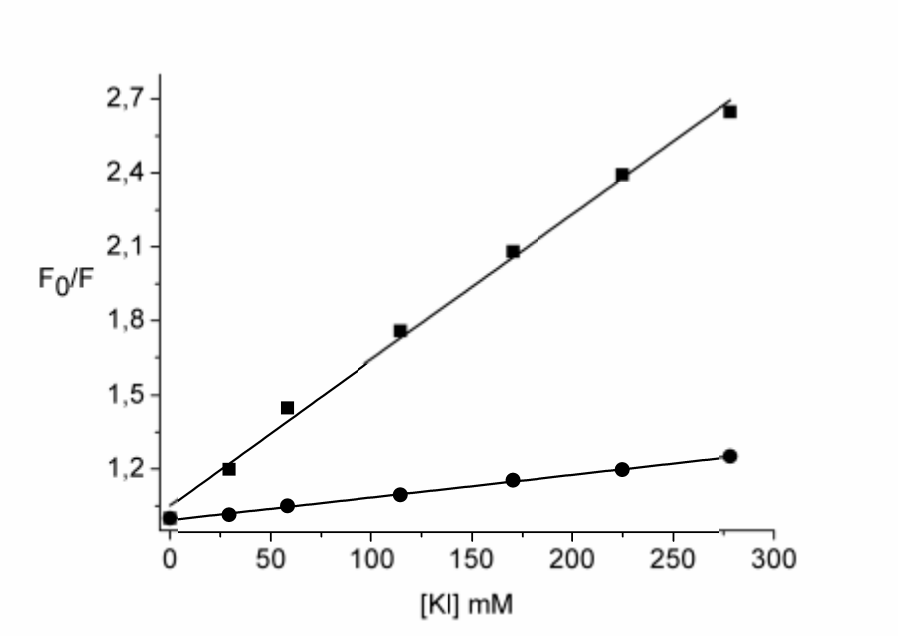

Figure 1.3: Fluorescence quenching of W20 LysM protein with potassium iodide. Square: in the absence of the ligand (peptidoglycan); tryptophan well accessible to KI. Circles: in the presence of the ligand; tryptophan less accessible to KI. Unpublished data.

tryptophan residues that are at distinct environments. If each of these residues shows a di erent accessibility to the quencher a downward curvature will be obtained.

1.1.4 Steady-state and time-resolved uorescence

Fluorescence spectroscopy measurements can be performed in either steady state or in time-resolved mode. In steady-state uorescence experiments, the uorophore is constantly illuminated and its uorescent properties investigated. In time-resolved measurements the uorophore is excited by a short pulse of light and the induced uorescence intensity (I(t)) is monitored in time. If the uorophore displays a single χ, I(t) can be described by equation 2a:

$$I(t) = I_0 \ \ e^{\ (\frac{t}{\ })} \quad (2a)$$

I_0 - The uorescence intensity at time t = 0.

χ - The uorescence lifetime of the uorophore.

If the uorophore displays multiple lifetimes, I(t) can be described by equation:

$$I(t) = \sum_i \phi_i \ \ e^{\ (\frac{t}{i})} \quad (2b)$$

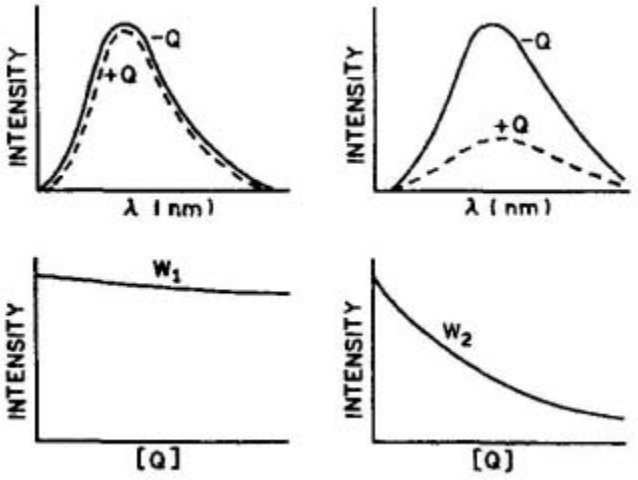

Figure 1.4: Fluorescence emission spectra and emission intensity dependence on [Q]: surface-accessible (right) and surface-buried (left) tryptophan residues in proteins. Data from [9].

with τ_i as the i^{th} lifetime with amplitude α_i.

The steady-state emission intensity is just an average of the signal collected in a time resolved measurement. As a result of this averaging, valuable information about the sample is lost. For example if two identical fluorophores are experiencing different microenvironments in a sample, it is not possible to assign their individual Q via steady-state fluorescent experiments (unless their emissions spectra are resolved). In time-resolved mode this is possible. If the fluorophore experiences different microenvironments, a set of different lifetimes is expected.

1.1.5 Fluorescence anisotropy

In an anisotropy measurement the fluorescent sample is excited with polarized light and the emission intensity is measured either parallel ($I_{\parallel}$) or perpendicular ($I_{\perp}$) to the orientation of the excitation light [3]. The fluorescence anisotropy (r), is defined as:

$$r = \frac{I_{\parallel} - I_{\perp}}{I_{\parallel} + 2I_{\perp}} \quad \text{(3a)}$$

with $I_{\parallel}$ and $I_{\perp}$ the fluorescence intensities when the emission polarizer is oriented parallel or perpendicular to the direction of the polarized excitation, respectively.

A fluorophore excited by polarized light also emits polarized light. However, if the

molecule can rotate while emitting, the direction of the emission will randomise, resulting in a lower anisotropy. In the case when no other processes than rotation result in loss of anisotropy, (r) can be described by the Perrin equation (equation 3b):

$$\text{Steady state anisotropy - } r = \frac{r_0}{1 + (\tau/\theta)} \quad \text{(3b)}$$

r_0 - fundamental anisotropy equal to the anisotropy of the fluorophore in the absence of rotational diffusion (at the selected excitation wavelength)
θ - rotational correlation time

The rotational correlation time of globular macromolecules can be described by equation 3c:

$$\theta = \frac{\eta V}{RT} = \frac{\eta M}{RT} \cdot (\nu + h) \quad \text{(3c)}$$

where η is the viscosity in poise (P), T is the temperature in K, R is ideal gas constant (8.31 J/molK), M is the molecular weight (g/mol), and (ν + h) is the specific volume (dm^3) of the macromolecule including its hydration shell.

Combining equations 3b and 3c gives a modified form of the Perrin equation:

$$\frac{1}{r} = \frac{1}{r_0} + \frac{\tau RT}{r_0 \eta V} \quad \text{(3d)}$$

The volume of the fluorescent macromolecule can be determined if the anisotropy of the macromolecule is measured over a range of temperatures or viscosities, and the data plotted in a graph with $\frac{1}{r}$ at the y-axis and $\frac{T}{\eta}$ at the x-axis. Extrapolation $\frac{T}{\eta}$ to 0 (a very high η) gives the fundamental anisotropy of the macromolecule ($\frac{1}{r_0}$) while the slope of the plot represents $\frac{\tau R}{r_0 V}$ (Figure 1.5).

Determination of the volume of a fluorescent macromolecule via the Perrin equation only works well if the τ of the fluorophore is not too different from θ. If the fluorophore can also rotate fast, independently of the rotation of the protein, a very low r value is obtained as $\frac{\tau}{\theta}$ in equation 3b becomes $>> 1$. As a result r will be minimally dependent on θ preventing a reliable determination of the size of the macromolecule. θ values can in general be determined more easily and accurately in time-resolved anisotropy experiments. In a time-resolved anisotropy experiment the decay of the anisotropy in time, r(t), is measured after excitation of the fluorophore with a polarized ultra-short laser pulse.

$$r(t) = \frac{I_{\parallel}(t) - I_{\perp}(t)}{I_{\parallel}(t) + 2I_{\perp}(t)} \quad \text{(3e)}$$

with $I_{\parallel}(t)$ and $I_{\perp}(t)$ as the detected emission intensity in time with the emission polarizer in parallel or perpendicular orientation relative to the excitation light source, respectively. The exponential decay of r(t) can be described using equation 3f:

$$r(t) = \sum_j r_{0j} \cdot e^{-\left(\frac{t}{\Phi_j}\right)} \quad \text{(3f)}$$

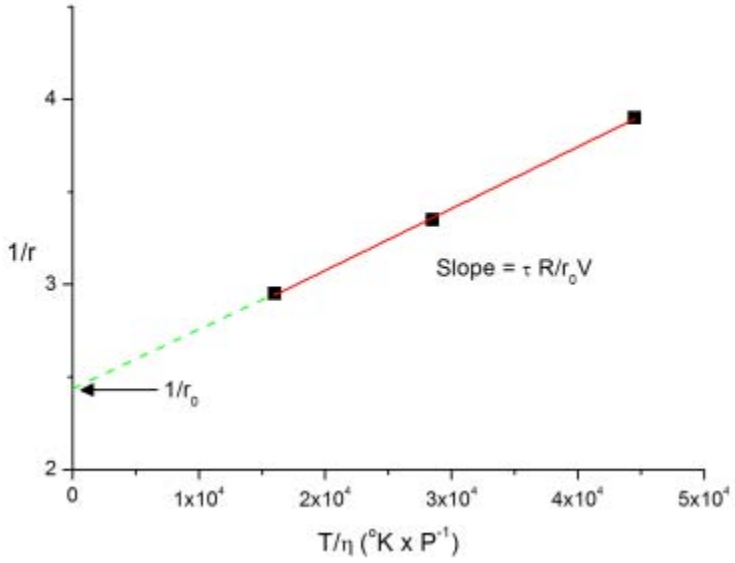

Figure 1.5: Perrin plot. Data from [10].

where Φ_j is the jst rotational correlation time with amplitude r_{0j}.

As the fluorescence anisotropy is sensitive to changes of the fluorophore rotation, these measurements are widely used to study the interactions between biological macromolecules (e.g. protein - ligand or protein-protein interactions).

1.1.6 Biochemical fluorophores

Biochemical fluorophores can be divided into two general classes, intrinsic and extrinsic fluorophores. Intrinsic fluorophores are those, which occur naturally. In proteins, the most interesting intrinsic fluorophore is the indole group of tryptophan, and it will be described in detail in the next section. Beside tryptophan also tyrosine and phenylalanine show fluorescent properties. The chromophore p-hydroxybenzylideneimidazolinone is formed from Ser65-Tyr66-Gly67 residues during folding of green fluorescent protein (GFP) from *Aequorea victoria* (Figure 1.6). It shows an intense absorption band at 395 nm and a minor one at 475 nm. Its emission peak is at 509 nm and the fluorescence quantum yield is very high, 0.79 [11]. Introduction of a single point mutation (S65T) in GFP was shown to result in an increase in Q and photostability, and a shift of the major excitation peak to 488 nm, without inducing a change in λ_{max} [12]. This improved GFP variant and

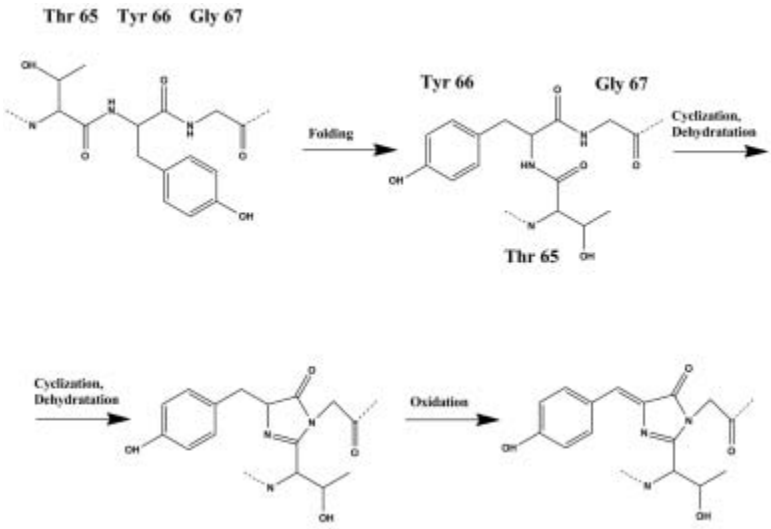

Figure 1.6: Autocatalytic fluorophore formation observed in green fluorescent proteins. Data from [12].

other GFP mutants have found widespread use in protein biochemistry and biology [13]. NADH, pyridoxal phosphate, riboflavine, FAD, and FMN are examples of fluorescent cofactors. When the biomolecule of interest is not fluorescent (e.g. lipids or DNA) or when the intrinsic fluorescence is not adequate, the biomolecule can be labelled with an extrinsic fluorescent probe. Numerous fluorophores are available for covalent and noncovalent labelling of proteins. For example, the fluorophore dansyl chloride (DNS-Cl) reacts with amino groups of proteins forming sulphon-amido linkages as the most important product of the reaction [14]. DNS-Cl can be excited at 350 nm, a wavelength where proteins do not absorb, and the emission maximum is near 520 nm [3]. Popular fluorophores which are commonly used to label proteins noncovalently are 1-anilino-8-naphthalene sulfonate acid (ANS) and 6-(p-toluidinyl)naphthalene-2-sulfonic acid (TNS) [15].

1.2 Protein fluorescence and tryptophan analogues

1.2.1 Tryptophan as an intrinsic protein fluorophore

The chemical modification of a protein can affect its structure and functional properties. Intrinsic fluorescent probes allow a biological system to be observed with no or minimal perturbations of the native structure. Tryptophan has been extensively used as intrinsic probe for studying protein structure, dynamics and local environment [16].

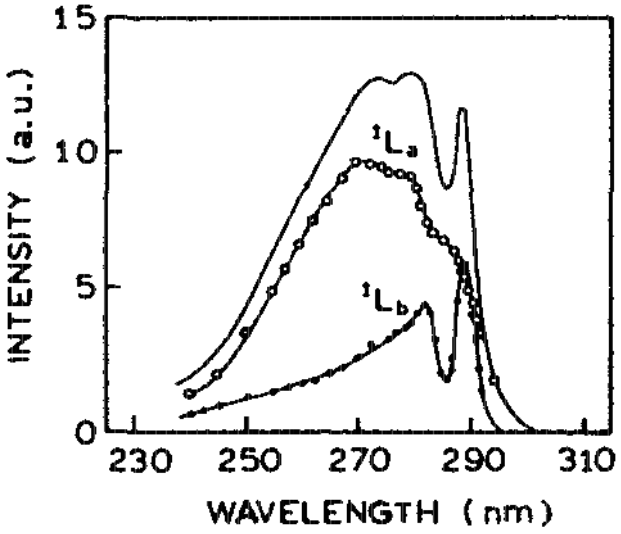

Figure 1.7: The anisotropy-resolved spectra of the ^1L_a (circles) and ^1L_b (dots) transitions of indole in vitrified propylene glycol. The absorption spectrum of indole is also shown. Data from [3].

Its absorption at wavelengths longer than 295 nm allows tryptophan to be excited independently of the other two aromatic amino acids, tyrosine and phenylalanine [10, 16]. Tryptophan is the least abundant amino acid residue in proteins[1] and when the protein contains only one Trp residue, interpretation of the spectral data is most straightforward. The photophysics of tryptophan is quite complex because the energies of the S_1 and S_2 excited states (Figure 1.1) overlap with each other. These two excited states, also known as ^1L_a and ^1L_b states [17], are responsible for the Trp absorption spectrum centred around 270 nm. Because of the overlap, specific excitation of either the ^1L_a or ^1L_b state is not possible, except when excitation takes place at the red edge of the spectrum, where only ^1L_a absorbs (see Figure 1.7). The ^1L_a state is always the fluorescent state of indole except for indole in vacuum, or when dissolved in perfluorohexane [18]. Excited-state conversion from ^1L_b to ^1L_a is known to be very fast compared to the fluorescence lifetime and ^1L_a is almost always the emitting state in proteins [3]. Only a small number of single Trp mutants of the transhydrogenase domain I protein are known to show emission from ^1L_b state [19].

The ^1L_a state has a much larger dipole moment than Trp in the ground state,

[1]Tryptophan is generally present at about 1 mol% in proteins [3].

while the dipole moment of the ^1L_b state is small and comparable to the ground state [20]. As a result of the large dipole moment of the fluorescing ^1L_a state, a large Stokes shift can be observed for Trp in a polar medium. Depending on the position of Trp in a protein, the λ_{max} ranges from 304 nm for a Trp in an occluded apolar microenvironment [20] to 355 nm for a Trp at a surface exposed position [21]. Beside λ_{max}, also the Q of Trp is highly sensitive for changes in the microenvironment. At 23 ^{0}C in aqueous solution at pH 7 the quantum yield of tryptophan is 0.14 and the emission maximum $\approx$ 350 nm [22], but the Q of Trp in a protein can vary from almost 0 to 0.35 [23]. Changes in Trp fluorescence can be used to monitor protein (un)folding, or conformational changes of protein-ligand interactions.

1.2.2 Tryptophan analogues

Alloproteins are proteins that contain non-canonical amino acids. Incorporation of Trp analogues in proteins was already described in the 1950s, and the aim of those studies was to elucidate metabolic pathways and the mechanism of protein synthesis [24, 25, 26]. In these first reports the alloproteins were not purified and characterized. The first description of a purified protein in which tryptophan was replaced by a Trp analogue (7-azatryptophan (7AW) and 2-azatryptophan (2AW)), was in 1956 [27]. In the 1970s several groups reported the incorporation of fluorotryptophans (FW) into proteins aiming to study the labelled proteins via ^{19}F NMR [28]. The introduction of artificially inducible promoters in the 1980s [29] as a common approach for protein expression opened possibilities for more proficient incorporation of Trp analogues. In the early 1990's protocols for the incorporation of Trp analogues in recombinant proteins were published [30, 31]. The new approach enabled incorporation efficiencies for 7AW, 5-hydroxytryptophan (5HW), and 5-fluorotryptophan (5FW) analogues between 50% and $\geq$95% [22]. Most work in this field is focused on the incorporation of these three analogues. 7AW and 5HW show significant red-shifted absorption spectra compared to Trp (Figure 1.8), which facilitates their selective excitation in the presence of Trp at wavelengths >305 nm. This selective excitation is also known as spectral edge excitation.

Besides the red-shifted absorbance of some Trp analogues, also other spectroscopic properties of Trp analogues can be exploited in protein chemistry. An attractive property of 7AW is its very high sensitivity of the quantum yield to a change in microenvironment. Free 7AW in neutral aqueous solutions is almost non-fluorescent (Q = 0.017) [32], while in a protein Q values of $\approx$ 0.5 have been reported [22]. 7AW in buffer features a 40 nm red-shifted emission maximum compared to Trp, [32, 33, 34]. The red-shift in emission maximum of 7AW was related to a larger dipole moment of the excited state compared to Trp [35]. The large sensitivity of 7AW for changes in microenvironment makes 7AW an interesting probe to examine protein-folding or protein conformational changes, also if

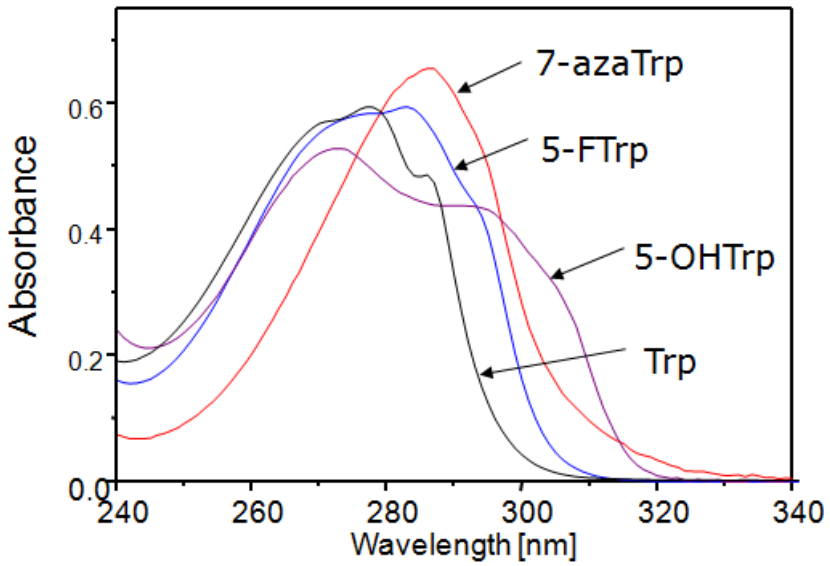

Figure 1.8: Absorption spectra of Trp and Trp analogues.

Trp-containing proteins are presented in the sample [22]. 5HW in neutral aqueous solution shows a quantum yield almost twice as high as Trp, 0.27 vs. 0.14, and features an emission maximum at 336 nm [32]. The blue-shifted emission maximum of 5HW, compared to Trp, has been related to ^1L_b being the emitting state of 5HW. The ^1L_b state has a much smaller excited-state dipole moment than ^1L_a and this explains the low sensitivity of λ_{max} for a change in 5HW microenvironment [22, 36]. In 5HW the ^1L_b state can be selectively excited at wavelengths above 310 nm [22]. Specific excitation of the ^1L_b state avoids depolarization of 5HW fluorescence emission due to internal conversion from ^1L_a to ^1L_b state. The higher intrinsic anisotropy value of 5HW compared to Trp, makes 5HW an attractive probe in fluorescence anisotropy measurements [30]. 5HW as free amino acid in aqueous solution at neutral pH shows a mono exponential decay. However, when incorporated in proteins two or three lifetimes are observed [37]. Another interesting Trp analogue is 5-fluorotryptophan. The fluorescence decay kinetics of a protein containing 5FW is more homogeneous than the decay kinetics of Trp at the same position. Often a monoexponential decay is observed [38], as well as a Q of ≈ 0.22 [39] making 5FW an attractive energy donor in time-resolved resonance energy transfer experiments [40]. Replacing Trp residues with 4FW converts the protein into a fluorescently "silent" protein, as 4FW is not fluorescent. Labelling a protein with 4FW allows monitoring the fluorescence of another Trp-containing protein in the same sample (for example in protein-protein

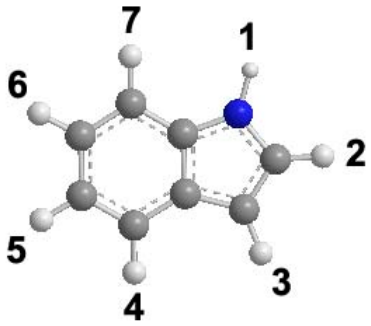

Figure 1.9: Numbering of indole substitution positions.

interaction studies) [41].

1.2.3 Aminoacyl-tRNA synthetase

During translation each of the 20 canonical amino acids is enzymatically coupled to its cognate tRNA in an aminoacylation reaction catalysed by an amino acid speci c aminoacyl-tRNA synthetase (aaRS). The tRNA coupled with its cognate amino acid (i.e. aminoacyl-tRNA) enters the ribosome where it participates in the decoding of the mRNA (via codon-anticodon interactions) and the attached amino acid is coupled to the nascent polypeptide chain via formation of a peptide bond. The coupling of the amino acid to its cognate tRNA is accomplished in a two-step reaction [42].

AA + ATP + aaRS aaRS AA-AMP + PPi (1)

aaRS AA-AMP + tRNA aaRS + AA-tRNA + AMP (2)

Acylation of tRNA with another amino acid than the cognate one can give rise to mutations in proteins [43]. Consequently, the substrate speci city of aaRS towards amino acid and tRNA is known to be very high, ensuring a high delity of the translation process. For example, although the structure of Phe compared to Tyr di ers by only a hydroxy group, its attachment to $tRNA^{Tyr}$ is highly discriminated by TyrRS [44]. The capability of the hydroxy group in Tyr to form two hydrogen bonds is maximally exploited during formation of the TyrRS Tyr complex. This binding energy is not available when Phe binds to TyrRS. The high substrate speci city of aaRS limits the incorporation of amino acid analogues to those structures showing high resemblance to natural amino acids.

1.2.4 Strategies to improve incorporation of amino acid analogues in recombinant proteins

Amino acid analogues can be incorporated in recombinant proteins, via an: (1) *in vitro* or (2) *in vivo* incorporation methodology. *In vitro* methods use a chemical aminoacylation step to label the tRNA in a cell-free translation system with the non-canonical amino acid. This is a versatile method for the incorporation of non-canonical amino acids, as also amino acids with side chain structures significantly different from the canonical amino acids can be introduced in proteins in this way. However limitations of this method are a low protein yield, and lack of natural posttranslational modifications of proteins [45].

In vivo methods for the incorporation of amino acid analogues use amino acid auxotroph strains (e.g. a Trp auxotroph), of which the expression system is under the control of a non-leaky promoter. In this method the growth medium, which contains the natural amino acid, is replaced with a medium containing the amino acid analogue of choice, before protein induction is started. Compared to the *in vitro* methods, this approach is experimentally simpler and often results in a similar recombinant protein yield as when a non-auxotrophic strain is used.

Aminoacyl tRNA synthetases (aaRS) were identified as "the bottleneck" for the incorporation of non-natural amino acids [46]. Much research in this field is directed toward engineering the aaRS activity to accepting non-canonical amino acids. Strategies used to extend the number of non natural amino acids which can be translated *in vivo* are: (1) redesigning of the amino acid binding pocket in aaRS [47], (2) overexpression of aaRS in the expression host [48, 49] and (3) creating an orthogonal aaRS/tRNA pair [50, 51, 52, 53]. Also, exploring the translation capability of a different expression host towards unnatural amino acids can result in the biosynthetic incorporation of new amino acid analogues [54]. In chapter 3 we explored the translation capability of *L. lactis* in order to incorporate Trp analogues in a recombinant protein, which can not be incorporated using *E. coli* as expression host.

1.3 LysM domain

The Lysin motif (LysM) is a widely spread motif in nature and its biological function is binding of peptidoglycan (PG) in the cell walls of bacteria or chitin-like compounds in eukaryotes [55]. The LysM was first discovered in the lysozyme of *Bacillus* phage ϕ29 [56]. Many proteins contain a LysM domain, which consists of only one LysM motif, such as the prophage amidase XlyA of *Bacillus subtilis* [57], while in others, LysM domain consists of several motifs [58, 59, 60, 61]. LysM motifs typically range in length from 44 to 65 amino acids residues [55]. LysM domain is separated from the catalytic part of the protein by a short spacer. Also, in proteins where the LysM domain consists of two or

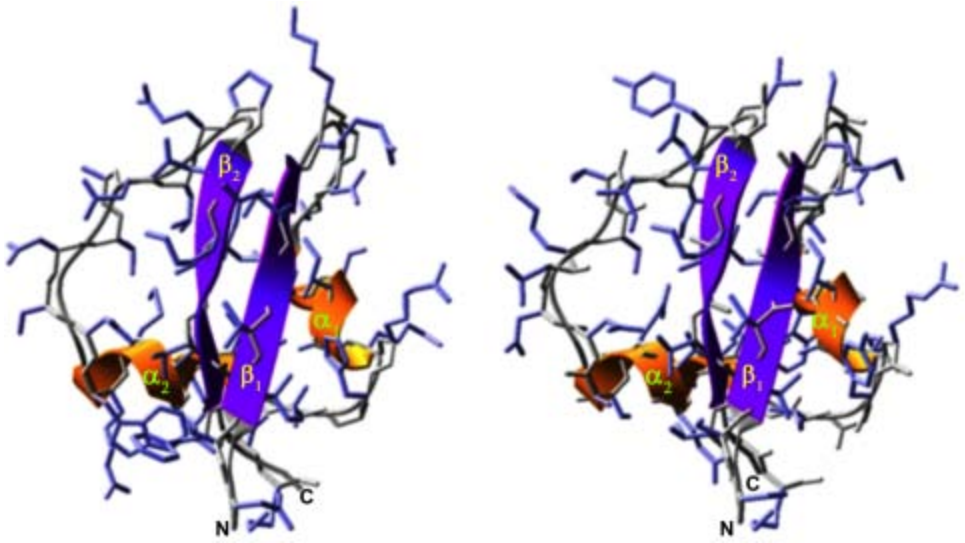

Figure 1.10: NMR structure of MltD-LysM2 of *E. coli* (Left panel) and the 3D model of AcmA-LysM1 (right panel). N- and C- termini, α helixes, and β strands are highlighted in the structure of MltD-LysM2 and the model of AcmA-LysM1.

more motifs, the motifs are separated by short spacers of 7 - 15 amino acid residues, rich in Ser, Thr, Asp or Pro residues, which may form a flexible region between LysM motifs [62]. LysM domains can be present at the N-terminal part of protein (e.g. LytF of *B. subtilis*), at the C-terminal part (e.g. AcmA of *L. lactis*) or present in the central part of a protein (e.g. XlyA of *B. subtilis*) [55].

1.3.1 The structure of LysM domain

To date only four LysM domain structures have been solved. The structure of the LysM domain from the lytic murein transglycosylase MltD of *E. coli* [63], the structure of the *B. subtilis* spore protein YkuD [61], a LysM structure belonging to the human hypothetical protein SB145 [64], and more recently, a CVNH-LysM lectin from the rice blast fungus *Magnaporthe oryzae* [65]. All four LysM structures show an $\alpha_1\beta_1\beta_2\alpha_2$ secondary structure with the two α-helices packing at the same side of an antiparallel β-sheet (Figure 1.10). Sequence alignment of LysM motifs from several species revealed that conserved amino acids are mostly positioned in turns between the secondary structure elements. These conserved amino acids probably play a role in the correct positioning of the α-helices and β-strands in LysM [55]. Characterization of the carbohydrate binding site using calorimetry and NMR techniques were employed to identify residues critical for lig-

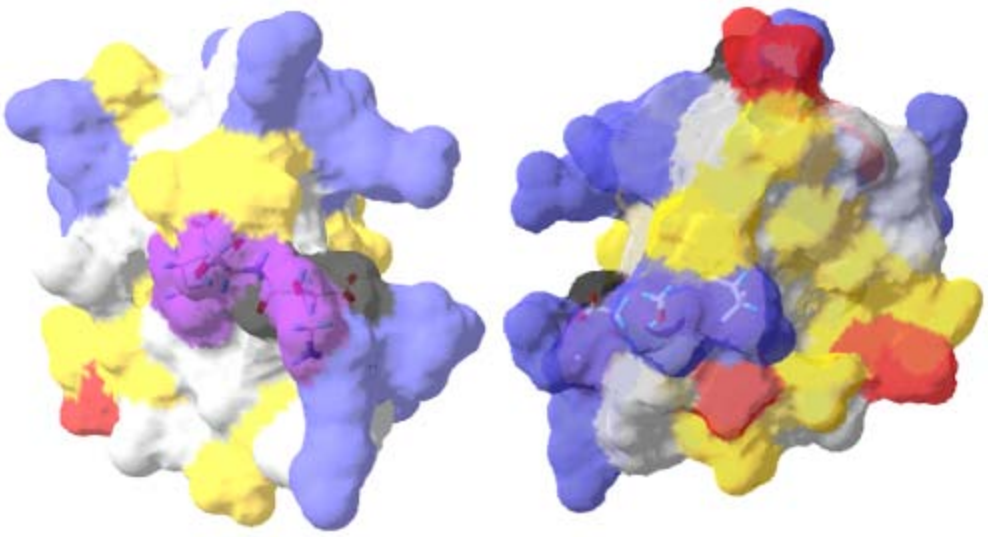

Figure 1.11: Structure of a MltD LysM motif showing the position of GDSL in the putative ligand binding site (left: front view, right: back view). G, S, and L are shown in pink and D in black.

and binding in two LysM motifs of the chitinase of *P. ryukyuensis* [66]. A shallow groove is formed by a cluster of hydrophobic residues at the N-terminal part of the α1 and the loop between the β1 and the α1, together with the C-terminal part of β2 and the loop connecting α2 and β2. Ohnuma et. al. proposed this shallow groove functions as ligand binding site of the LysM motif [66]. Conserved Gly10 and Gly21 residues are found in short turns between the β-strands and α-helices, the highly conserved Asp28 (nomenclature of Buist et al. [55]) seems to form a turn at the end of the second α-helix. A highly conserved G D T/S L sequence is also present in LysM motifs [55] (Figure 1.11) and it has been proposed that Asp in this sequence plays a role in ligand binding, as well as the conserved Thr/Ser and Gly residues [67].

1.3.2 LysM domain of the N-acetylglucosoaminidase AcmA of *L. lactis*

The LysM domain from N-acetylglucosaminidase (AcmA) of *L. lactis* is the most intensively studied LysM domain [62, 68, 69, 60, 70]. AcmA is a 40.3 kDa cell wall hydrolase of *L. lactis*, involved in cell separation after cell division [62]. It consists of two motifs, an N-terminal glucosaminidase domain, and a C-terminal cell-wall binding LysM domain. The LysM domain of AcmA consists of three highly homologous motifs. The

size of each motif is 45 amino acids, and they are separated by nonhomologous spacer sequences [62]. Binding of AcmA to *L. lactis* cells was found to be highly dependent on the number of LysM motifs. Two of the three LysM motifs are needed for efficient binding of AcmA to the cell-wall [69]. Steen et al. showed that the LysM domain of AcmA binds to many gram-positive bacteria with different PG structures [60]. The only common part of all analysed PG structures is a disaccharide building block consisting of N-acetylglucosamine and N-acetylmuramic acid. This result suggests that the AcmA LysM domain most likely binds to this component of the PG [55]. Immunofluorescence microscopy revealed that the AcmA LysM domain interacts with specific loci on the cell surface [60]. Chemical treatment of *L. lactis* cells and cell-walls using trichloracetic acid (TCA) removes components responsible for preventing LysM domain recognition. This treatment yields so called **b**acterium **l**ike **p**articles (BLPs). Cells and cell-walls treated this way show a much higher binding capacity toward LysM domains [71, 72]. BLPs found application in vaccines through the intranasal route, which is an attractive alternative to conventional intramuscular injection vaccines [73].

1.4 Thesis outline

Because of its attractive spectroscopic characteristics, Trp is often used as an intrinsic fluorophore in proteins. Its fluorescence emission maximum and quantum yield are strongly dependent on the microenvironment and can provide us with information about protein structure or protein - ligand interactions [16].

In biochemical systems where more than one Trp-containing protein is present, the interpretation of the Trp fluorescence data can be difficult or even impossible. One way to overcome this limitation is the biosynthetic replacement of a specific Trp by a Trp analogue with different spectroscopic properties. Trp substitution by a Trp analogue with different spectroscopic properties leads to spectrally enhanced recombinant proteins [22].

In *Chapter 2* four functional single-Trp LysM mutants and one double Trp LysM mutant were constructed and biosynthetically labelled with 7AW or 5HW. These Trp analogues feature red-shifted absorption spectra, and enabled monitoring of the LysM - ligand interaction in media with a Trp background. The method described in this chapter can be used for the detection of low levels of peptidoglycan or microbes in solutions.

In *Chapter 3* an expression system is presented that allows efficient incorporation of chloro- and bromo- atoms containing Trp analogues in alloproteins at high expression levels using a *Lactococcus lactis* Trp auxotroph strain. Coexpression of the enzyme tryptophanyl-tRNA synthetase of *L. lactis* (lacTrpRS) was essential for the biosynthetic incorporation of these analogues and also for incorporating 5,6 difluoroTrp. The presented expression system features the most relaxed specificity for Trp analogues reported to date and gives a high alloprotein yield.

In *Chapter 4* the intrinsic anisotropy of free 5HW and of four proteins labelled with 5HW was exploited in order to clarify which state emits in 5HW, the ^1L_a or ^1L_b state. The obtained results provided the first experimental evidence that ^1L_a can be the emitting state for this Trp analogue incorporated in a protein.

Chapter 2

Monitoring LysM-ligand interactions via tryptophan analogue fluorescence spectroscopy

Dejan M. Petrović, Kees Leenhouts, Maarten L. van Roosmalen, Fenneke KleinJan, Jaap Broos

Published in *Anal. Biochem.*, 2012, Volume: 428, page: 111-118.

2.1 Abstract

The lysin motif (LysM) is a peptidoglycan-binding protein domain found in a wide range of prokaryotes and eukaryotes. Various techniques have been used to study the LysM-ligand interaction but a sensitive spectroscopic method to directly monitor this interaction has not been reported. Here a tryptophan analogue fluorescence spectroscopy approach is presented to monitor the LysM-ligand interaction using the LysM of the N-acetylglucosaminidase enzyme of *Lactococcus lactis*. A 3D model of this LysM protein was built based on available structural information of a homologue. This model allowed choosing the amino acid positions to be labelled with a Trp analogue. Four functional single-Trp LysM mutants and one double Trp LysM mutant were constructed and biosynthetically labelled with 7-azatryptophan or 5-hydroxytryptophan. These Trp analogues give red-shifted absorption spectra, enabling the monitoring of the LysM-ligand interaction in media with a Trp background. The emission intensities of four of the five LysM constructs were found changing markedly upon exposure to either *L. lactis* bacterium-like particles or purified peptidoglycan as ligands. The method reported here is suitable to monitor LysM-ligand interactions at (sub)micromolar LysM concentrations and can be used for the detection of low levels of peptidoglycan or microbes in solutions.

2.2 Introduction

Peptidoglycan (PG) is a biopolymer consisting of glycan chains of alternating N-acetylglucosamine and N-acetylmuramic acid residues, cross-linked by peptide bridges. Its presence in the bacterial cell wall provides structural strength to the cell, and counteracts the osmotic pressure of the cytoplasm. For growing and dividing, bacteria produce enzymes that can hydrolyse bonds in the peptidoglycan matrix [74]. These enzymes are secreted and attached in a non-covalent manner to the cell wall via specific protein domains, Lysin Motif (LysM) domains [55]. The LysM domain is separated from the catalytic part of the enzyme by a short spacer, it can appear either at the N-terminus or at the C-terminus of the proteins, and sometimes is present in the central part of proteins [55]. The LysM domain is mostly found in enzymes that degrade bacterial cell walls [75]. A LysM containing protein can hold in between one to twelve LysM motifs, separated from each other by short spacers [76, 58, 59]. A LysM motif typically contains 42 to 65 amino acid residues and spacers usually consist of 7 - 33 amino acid residues which may form a flexible region between LysM motifs [62]. The structures of several LysM motifs have been determined by nuclear magnetic resonance (NMR) spectroscopy or X-ray crystallography: MltD of *E. coli*, YkuD from *Bacillus subtilis*, human hypothetical protein SB145 and more recently a CVNH-LysM lectin from the rice blast fungus *Magnaporthe oryzae* [64, 65, 63, 61]

More than 4000 proteins of both prokaryotic and eukaryotic origin have been found to contain a LysM domain [55]. One of the best-characterized LysM domains is the one from N-acetylglucosaminidase, AcmA, of *Lactococcus lactis* [62, 68, 70, 69]. AcmA contains three LysM motifs at the C-terminal end (Figure 2.7). The primary sequence of these motifs differs slightly. Binding studies using the C-terminal part of AcmA containing the three LysM motifs identified PG as the component of the cell wall to which LysM binds [60]. To achieve sufficient affinity for the cell wall at least two LysM motifs are needed [69]. Despite an increasing number of reports in which PG is identified as the LysM binding component [57, 58, 59, 60, 69, 55] the mode of its interaction at the molecular level is still unknown.

Techniques that have been used to study the interaction between LysM domains and cell walls or PG include halo formation, cell separation and sedimentation [69, 68], immunofluorescence [60], isothermal calorimetry, NMR [66], and atomic force microscopy [77]. A spectroscopic method in which only minute amounts of LysM are needed and allowing the direct monitoring of the binding event has not been presented. Such a method will not only be useful to find new ligands but could also find application in a biosensor for the detection of PG or microbes with LysM as molecular recognition element. This work a fluorescence methodology is presented to monitor the binding interactions between LysM and its substrates, by taking advantage of the intrinsic fluorescence properties of

LysM domain. To make this possible, we created four single Trp LysM mutants and one LysM construct with two Trp residues. Each recombinant protein consists of two LysM motifs (LysM tandem). An enzyme-linked immunosorbent assay (ELISA) was developed to verify the binding functionality of the newly constructed LysM tandems. To monitor interactions with cell walls or PG in the presence of other proteins, we biosynthetically labelled the LysM tandem with Trp analogues featuring a red-shifted absorption. The red-shifted absorption spectra allow specific excitation in a Trp background. 7-azatryptophan (7AW) and 5-hydroxytryptophan (5HW) show this feature [37, 78, 79, 22]. Recently, we reported the use of a *L. lactis* tryptophan auxotroph as host to incorporate 7AW and 5HW tryptophan analogues [54], and this host was used in this study.

Mixing μM concentrations of 7AW or 5HW labelled LysM tandems with purified PG [80] or with acid treated *L. lactis* cells called bacterium-like particles (BLPs) [71, 72] resulted in marked changes in the fluorescence emission of most LysM tandem constructs investigated. The developed method offers great potential to study the interactions between LysM motifs and their ligands in more detail.

2.3 Materials and methods

2.3.1 Chemicals

D,L-7AW and L-5HW were obtained from Sigma-Aldrich.

2.3.2 LysM ligands

PG was purified from lyophilized cells of *Brevibacterium lactofermentum* as described previously [80]. Briefly, lyophilized cells of *B. lactofermentum* were resuspended in 1% sodium dodecylsulfate (SDS), stirred at room temperature for 12 h, and then centrifuged. This procedure was repeated 16 times. SDS was removed from the suspension by repetitive washing with water. Proteins in the suspension were subsequently digested using trypsin from porcine pancreas (Sigma-Aldrich). The trypsin was inactivated by shaking the suspension at 90 °C for 20 min and was subsequently washed six times with an aqueous solution of 5 $\times 10^{-4}$ M ethylenediaminetetraacetic acid (EDTA) followed by repetitive washing with water. In this protocol, the cells are not treated with strong acid, a step known to remove cell wall polysaccharides, as demonstrated for *L. lactis* cells [81]. Because this sample likely contains some polysaccharides other than PG, we refer to it as "purified cell walls" in this work.

The PG chain length distribution of the purified cell walls was not determined and has not been reported for *B. lactofermentum*. The obtained distribution depends on the isolation procedure and the type of cells used. For example, the protocol employed in this

work results in an average PG chain length of approximately 100 hexosamines if *Spirillum serpens* cells are used [80], whereas *L. lactis* cells, following a different procedure give 26% to 43% of PG chains with more than 50 hexosamines [82].

BLPs were produced exactly as described previously [71, 72]. Briefly, *L. lactis* MG1363 cells from a fresh overnight culture were diluted 100-fold in 500 ml of fresh GM17, and the standing culture was left to grow for 16 h at 30 °C. Cells were collected by centrifugation (10 min, 13,000 g) and washed once by addition of 250 ml of sterile distilled water, vortexed, and centrifuged. Subsequently, 100 ml of 0.6 M trichloroacetic acid (TCA) was added to the pellet, and the cell suspension was placed in boiling water for 30 min in a tube under atmospheric pressure. Next, the cells were washed three times in 250 ml of sterile phosphate-buffered saline (PBS) with vigorous vortexing. After the last washing step, cells were taken up in 50 ml of PBS. The number of BLPs per millilitre was determined microscopically with a Burker-Turk counting chamber.

Because both the purified cell walls and BLP samples are not uniform in composition, their concentration cannot be expressed in molarity concentration units, and so milligrams per millilitre (mg/ml) was used instead.

2.3.3 General DNA techniques

Standard recombinant DNA techniques were performed as described previously [83] or as specified by the manufacturers. Enzymes and buffers were purchased from BioLabs-New England or Roche.

Plasmid pPA40 (laboratory collection, table 1) containing the gene fragment encoding the most N-terminal AcmA LysM motif, AcmA-LysM1, including signal sequence, 14 amino acid spacer, and a "c-myc" region encoding an epitope for immunodetection at its N-terminus, was used to create Trp-less AcmA-LysM1. Trp at position 14 in AcmA-LysM1 was mutated to Tyr via a PCR using the Quick Change Site-Directed Mutagenesis kit (Stratagene) and the following primers: fw, 5'-ACC GTC AAA TCT GGT GAT ACT CTT **TAT** GGA ATC TCA CAA AGA TAT and rev, 5'-C ATA TCT TTG TGA GAT TCC **ATA** AAG AGT ATC ACC AGA TTT GAC GG. The PCR product was treated with the restriction enzymes NcoI and XhoI and ligated into a nisin inducible expression-secretion vector derived from pNZ8048 [84], resulting in plasmid pPD600 (Table 1).

The DNA sequences for four single Trp mutants of the AcmA-LysM1 domain, including a spacer at the N-terminal end, were chemically synthesized. Trp14 was replaced by Tyr and a Trp codon was introduced at corresponding codon positions of amino acid residues 5, 15, 20, and 39, respectively. Each synthetic fragment was fused, using Esp3I and HindIII restriction sites, to the 3' end of the Trp-less AcmA-LysM1 gene in plasmid pPD600, yielding four single Trp LysM tandem constructs (Figure 2.7).

The double Trp LysM tandem, containing two fused AcmA-LysM1 motifs, each har-

bouring Trp14, was created as described previously [71].

Electrotransformation of Trp auxotroph *L. lactis* strain PA1002 [54] was carried out as described previously [85] using a Bio-Rad Gene Pulser (Bio-Rad). Nucleotide sequence analysis and DNA synthesis were performed by BaseClear (Leiden, The Netherlands).

2.3.4 Expression of LysM tandem constructs

L. lactis Trp auxotroph strain PA1002, harboring the plasmid containing the gene of the LysM tandem construct, was grown overnight in GM17 broth (M17, Oxoid) supplemented with 0.5% (w/v) glucose and 5 μg/ml of chloramphenicol at 30 °C [86]. Subsequently, fresh GM17 with 5 μg/ml of chloramphenicol was inoculated (1:20) with the overnight culture and grown until an OD_{600} of 0.8 was reached. The cells were harvested by centrifugation at 8.000 × g for 10 min at 30 °C, washed three times with PBS, and resuspended in 50 ml CDM (chemically defined medium) [87], supplemented with 0.5% (w/v) glucose and 1 mM of all amino acids, except Trp. After a starvation period of 30 min at 30 °C, nisin and 1 mM 7AW or 5HW was added as described [54]. The cells were subsequently incubated for 18 h at 30 °C.

2.3.5 Protein purification

The LysM tandem protein (20.1 kDa) is secreted and it is the most abundant protein in the culture supernatant. After centrifugation, ammonium-sulphate (AS) was added to the culture supernatant to 30% saturation, and the pH was adjusted to 7.1. This solution was loaded on a 5 ml HiTrap Phenyl HP column (GE Healthcare) and washed with 5 column volumes of 30% AS in 50 mM Na-Phosphate buffer, pH 7.1, using FPLC (Äkta fplc, Uppsala, Sweden) at 4 °C and a flow rate of 1.5 ml/min. The LysM tandem protein was eluted using a 15 ml gradient from 30% to 0% AS saturation in 50 mM Na-Phosphate buffer, pH 7.1. Fractions containing the protein of interest were dialyzed against 100 mM Na-Phosphate buffer, pH 7.1 at 4 °C. The protein purity was > 95% according to SDS-PAGE analysis. Protein concentrations were determined using a Bradford assay with BSA as standard.

2.3.6 Fluorescence

Steady-state fluorescence spectra were recorded with a Fluorolog-3 fluorimeter (Instruments S.A. Inc., Edison, New Jersey, USA). A protein concentration of 0.5 μM in 125 μl PBS buffer (pH 7.4) was used. The 7AW- and 5HW-containing proteins were excited at 305 nm or 310 nm, respectively. Excitation and emission slits were set at 1.25 nm and 4 nm, respectively, and 3 × 3 mm quartz cuvettes were used. Fluorescence emission was measured from 320 nm to 500 nm at 23 °C. All spectra were corrected for buffer and

instrument response. Spectra were recorded two or three times, and the variation between the integral values were found to be less than 5%.

2.3.7 Modelling and computational docking of an AcmA LysM motif

The program "WhatIf" [88] was used to generate a structural model of AcmA-LysM1, using an alignment with the sequence of the second LysM motif of MltD from *E. coli* (MltD-LysM2) of which the structure has been solved by NMR spectroscopy [63].

The program AutoDock 3.05 [89] was used to predict the location of the binding site of AcmA-LysM1 using GlcNac-MurNac-Ala (N-acetyl-D-glucosamine-N-acetyl-muramic acid-Alanine) as a flexible ligand with 19 rotatable bonds. The following local-global alignment (LGA) parameters were used: initial population = 50; maximum number of energy evaluations = 5×10^6; maximum number of generations = 27,000; The GridBox-size ($100 \times 100 \times 100$), and grid point spacing (0.350 Å) were chosen such that the entire AcmA-LysM1 structural model fits in the GridBox.

2.3.8 Enzyme-linked immunosorbent assay (ELISA)

BLPs were washed in coating buffer (100 mM $NaHCO_3$, pH 9.6), and suspended to 2.5×10^9 particles per ml. Purified PG was diluted in coating buffer to 100 μg/ml. Hundred μl aliquots of the BLP suspension, or the PG solution, was added to the wells of a polystyrene ELISA plate. The plate was incubated overnight at 37 °C; unsealed when BLPs were coated and sealed when PG was coated. The wells were blocked by incubation with 1.5% gelatin in 1% Tween in Tris buffered saline (TTBS) for 1.5 hours at 37 °C, and subsequently washed with TTBS. Fifty μl of LysM tandem construct solutions, with concentrations ranging from 1×10^{-4} to 1×10^{-1} mg/ml, were added followed by incubation for 2 hours at 37 °C, and subsequently washed with TTBS. Hundred μl of 2,500 times diluted myc antibody, labelled with horseradish peroxidase was added followed by a 2 h incubation, two washing steps with TTBS, and a single washing step with 100 mM Na-acetate buffer pH 5.0. For detection, a 100 μl solution containing 1 mg/ml o-phenylenediamine, and 1% H_2O_2 was used. After 5-30 min, the reaction was stopped by adding 50 μl of 1M H_2SO_4. The absorbance was measured at 410 nm.

2.4 Results

2.4.1 Molecular modelling of a LysM motif of AcmA

The 3D structures of the AcmA LysM motifs from *L. lactis* have not been determined. However the structures of LysM motifs from two prokaryotes have been reported, the *B. subtilis* YkuD LysM domain [61] and the *E. coli* MltD LysM motif (MltD-LysM2) [63]. The overall sequence identity between AcmA-LysM1 and MltD-LysM2 is 30% (Figure 2.1) and this structure was used to build a model of AcmA-LysM1. The genome sequence of *L. lactis* IL1403 has been reported and contains, besides AcmA, three other genes encoding cell wall hydrolases with an active site homologous to that of AcmA: *acmB*, *acmC* and *acmD*. AcmD shows the highest sequence homology to AcmA [90] and the sequence of all three AcmD-LysM motifs, the MltD-LysM2 motif and the three AcmA LysM sequences were used in an alignment. The alignment revealed a well known highly conserved sequence, Gly10-Asp11-Tyr12-Leu13, in the AcmA LysM motifs, as well as a number of conserved hydrophobic residues (Figure 2.1). Asp11 is conserved in most of the LysM motifs, and it has been proposed that it interacts with ligand [55]. The results presented in figure 2.1, combined with the MltD structure, resulted in a model of the AcmA-LysM1 structure presented in figure 2.2.

2.4.2 *In silico* docking with carbohydrate substrate

Computational flexible docking techniques have been used to successfully predict protein-carbohydrate interactions [91, 92]. The computer program AutoDock is capable of automated docking of a flexible ligand to a nonflexible macromolecular target of known structure [93, 94]. Bacterial PG consists of chains of GlcNac-MurNac disaccharide repeats. The polysaccharide chains are interconnected with a peptide bridge attached via the MurNac moiety. A part of this repeating structure, the GlcNac-MurNac disaccharide with the first alanine residue of the peptide bridge, GlcNac-MurNac-Ala (N-acetyl-D-glucosamine-N-acetyl-D-muramic acid-alanine) was used in a flexible docking procedure to predict the potential binding site(s) of the AcmA LysM domain. The three energetically most favourable docking results resulting in final docked energies close to -11 kcal/mol are shown in figure 2.3. The docking results suggest that the region containing the first α-helix and also the loop after the first β-sheet (Figure 2.2) are important for substrate binding, possibly at both sides. This prediction is in good agreement with the position of the binding site of MltD-LysM proposed by Bateman and Bycroft [63], Ohnuma et al. [66] and Leonardus et al. [65]. The docking model presented in figure 2.3 served as basis to design single Trp mutants of AcmA-LysM1 by selecting residues Tyr5, Gly15, and Tyr20 which are close to the putative binding site. Tyr39 was also changed to Trp because it is at a distant position from the putative binding groove. According to the docking results

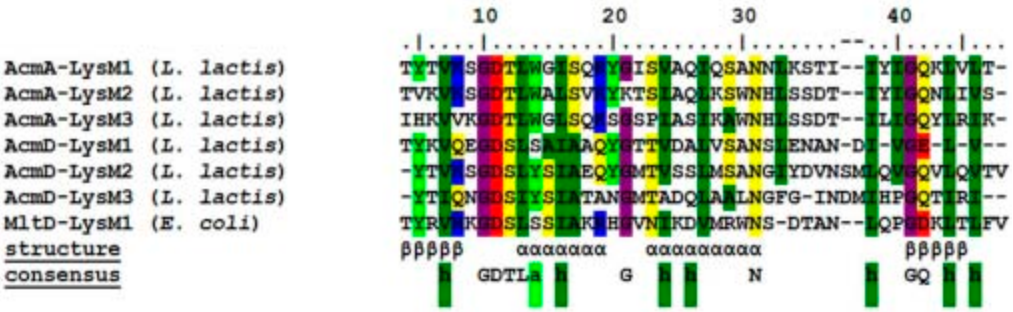

Figure 2.1: Alignment of the amino acids sequences of all three LysM motifs of AcmA (*L. lactis* MG1363), all three LysM motifs of AcmD (*L. lactis* IL1403) and the second LysM motif of MltD (*E. coli*). The secondary structure (= beta-sheet, = alpha-helix) and the consensus sequence (h = hydrophobic, p = polar, a = aromatic) are indicated below the alignment. In the alignment, amino acids are shaded for similarity (yellow = polar; green = hydrophobic; light green = aromatic; blue = positively charged; red = negatively charged; purple = Gly).

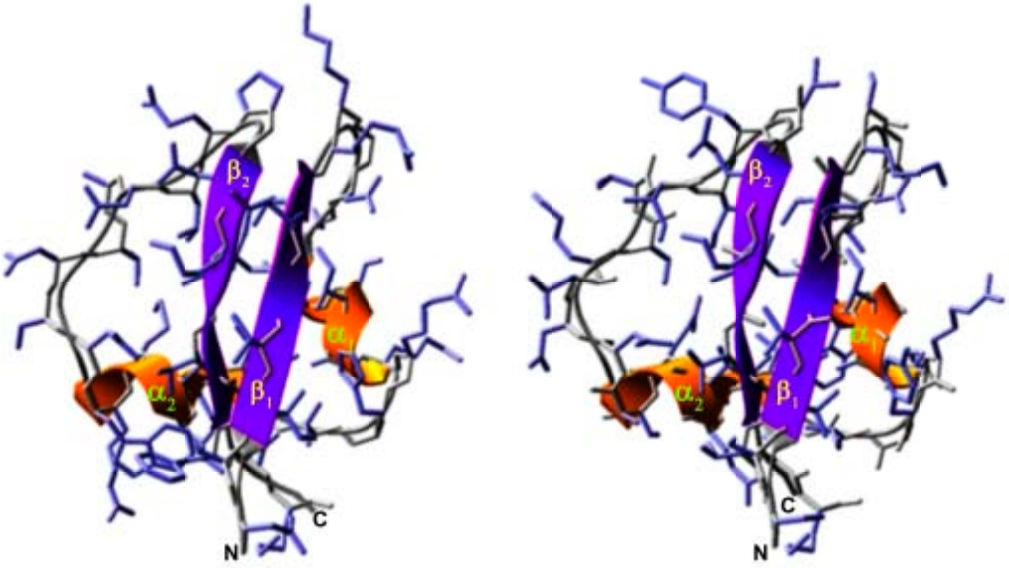

Figure 2.2: NMR structure of MltD-LysM2 of *E. coli* [63] (Left panel) and the 3D model of AcmA-LysM1 (right panel). N- and C- termini, helixes, and strands are highlighted in the structure of MltD-LysM2 and the model of AcmA-LysM1.

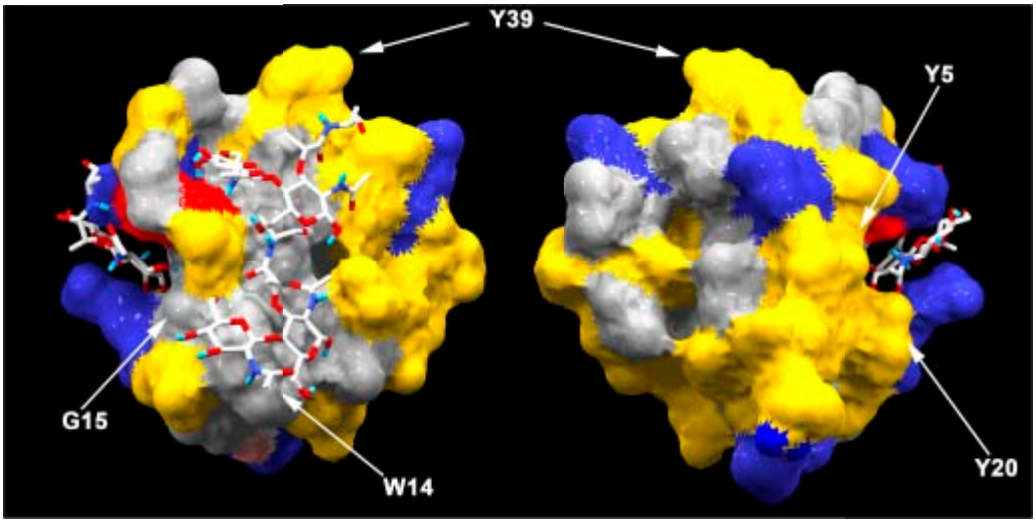

Figure 2.3: Putative binding site of GlcNac-MurNac-Ala to AcmA-LysM1 according to *in silico* docking experiments (left panel - front view; right panel - back view). The three energetically most favourable docking results with GlcNac-MurNac-Ala as substrate are presented. Color codes of the amino acids at the surface: yellow = polar; gray = hydrophobic; blue = positively charged; red = Asp31 (only negatively charged residue present). Locations of the residues mutated to Trp in this work are indicated by white arrows.

we expect that the microenvironment of Trp39 does not change upon ligand binding and this mutant can serve as negative control.

2.4.3 Enzyme-linked immunosorbent assay for monitoring binding properties of LysM tandems

Only two of the three LysM motifs of the AcmA LysM domain are needed for cell wall binding. The AcmA LysM domain harboring all three LysM motifs gave only a slightly higher binding a nity [69] An ELISA was developed to test the functionality of the single-Trp LysM tandems. In this assay we take advantage of an epitope tag (c-myc) introduced at the N-terminus of the LysM tandem construct (supplementary gure 1.7). A nity constants for the BLPs or puri ed cell walls and LysM tandem protein interaction cannot be generated (i) because of the nonuniform composition of the ligands and (ii) because BLPs and puri ed cell wall molecules, containing a large number of hexosamine units, can potentially bind more than one LysM tandem protein, so that no conclusion can be drawn about the stoichiometry of the interaction.

Wells of polystyrene ELISA plates were coated with BLPs or puri ed cell walls.

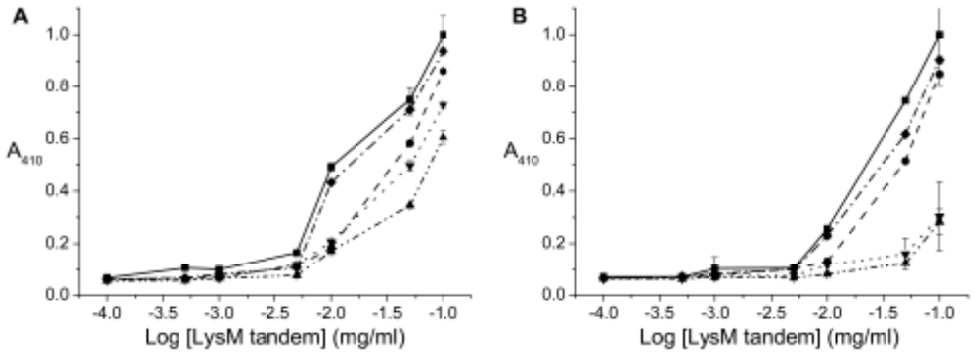

Figure 2.4: Detection of the binding a nity of 7AW-labelled LysM tandem mutants via ELISA assay. Wells were coated with (A) BLPs or (B) PG. wild-type double LysM tandem; - - - W5 LysM tandem; - - W15 LysM tandem; W20 LysM tandem and - - W39 LysM tandem.

Next, the LysM tandem was introduced in the wells and after washing, LysM tandems bound to the substrate were detected using monoclonal anti c-myc antibodies labelled with horseradish peroxidase. When ELISA plates were coated with 2.5 10^9 BLPs/ml, or 100 g/ml puri ed cell walls, a linear response was measured at 410 nm when 0.01 - 0.1 mg/ml LysM tandem proteins were used. Results of these ELISAs showed that all single Trp LysM tandems retained their functionality, but exhibited a lower binding a nity towards BLPs and puri ed cell walls compared to the double Trp LysM tandem that contains a Trp at the wild type position (Figure 2.4). The lowest binding a nity was observed for the W15 and W20 LysM tandems, whereas the W5 and W39 LysM tandems show only a slightly lower binding a nity toward BLPs and puri ed cell walls compared to the double Trp LysM tandem. The observed di erences in binding a nity indicate that the engineered positions in single Trp LysM tandems have an e ect on ligand binding. Due to the limited LysM solubility in the used bu er, we were not able to saturate all binding sites.

2.4.4 Monitoring interactions between LysM tandems and BLPs via uorescence

7AW was incorporated into the W5, W15, W20, and W39 single-Trp LysM tandems, using a published protocol known to result in >95% 7AW incorporation e ciency [54]. Similarly, the W15 and W20 LysM tandems and the double Trp LysM tandem constructs were labelled with 5HW. For unknown reasons the W5 and W39 LysM tandems could not be well expressed in the presence of 5HW. The puri ed LysM tandems were titrated

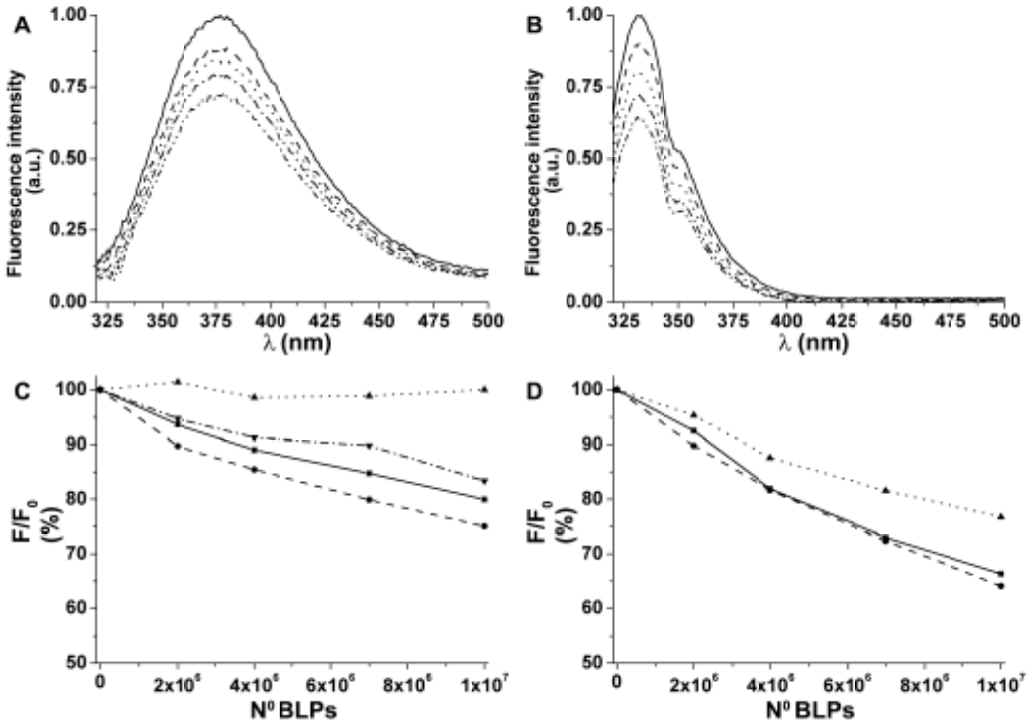

Figure 2.5: Fluorescence experiments with W20 LysM tandem.
(A) Fluorescence spectra of W20 LysM tandem labelled with 7AW in the presence of various amounts of BLPs (0; - - - 2 10^6; 4 10^6; - - 7 10^6 and - - 1 10^7 BLPs).
(B) Fluorescence spectra of W20 LysM tandem labelled with 5HW in the presence of various amounts of BLPs (0; - - - 2 10^6; 4 10^6; - - 7 10^6 and - - 1 10^7 BLPs).
(C) Dependence of the uorescence intensity of 7AW labelled LysM tandems to binding of BLPs (W5 LysM tandem; - - W15 LysM tandem; - - - W20 LysM tandem and W39 LysM tandem).
(D) Dependence of uorescence intensity of 5HW labelled LysM tandems to binding of BLPs (w.t. double LysM tandem; W5 LysM tandem; - - - W20 LysM tandem).

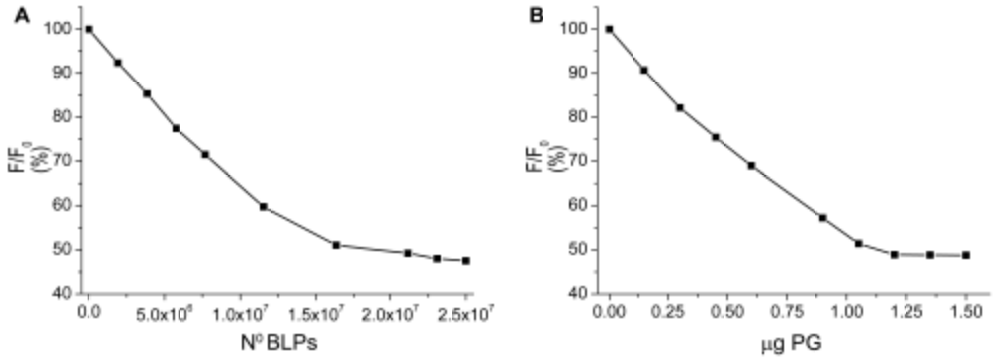

Figure 2.6: Titration curves of 5HW labelled W20 single Trp LysM tandem titrated with BLPs (A) or PG (B).

with BLPs to study the suitability of the Trp analogue to monitor the binding of ligand. Di erent amounts of BLPs (2 10^6 to 10^7 particles) were mixed in solution with 1.25 g of LysM tandem. Upon introducing 10^7 BLPs in the solution, the uorescent intensity decreased 15%, 20%, and 25% for the 7AW labelled W5, W15, and W20 LysM tandems, respectively (Figure 2.5). The uorescent signal of W39 LysM tandem labelled with 7AW did not change signi cantly (3%) when mixed with BLPs. Of all 7AW and 5HW labelled LysM tandems investigated, the emission intensity of the 5HW labelled W20 LysM tandem and the double Trp LysM tandem showed the highest sensitivity for BLP binding ($\gg$35% change when 10^7 BLPs were used). When the W20 single Trp LysM tandem labelled with either 7AW or 5HW was thermally inactivated before the titration experiment (30 min at 100 C), only a 3 - 5% change in uorescence was observed. This experiment con rmed that the change in uorescence correlates to LysM-BLP binding events and is not caused by an unspeci c quencher present in BLP. The 3D structures of the investigated LysM tandem proteins are not known; therefore, it is not possible to explain at the molecular level the mechanism of the observed changes in uorescence intensity on ligand binding.

The emission maximum of all four 7AW labelled single Trp LysM tandems is 388 1 nm, and of the three 5HW labelled LysM tandems 334 1 nm. These emission maxima are typical for 7AW or 5HW exposed at the protein surface [32]. Indeed, in our AcmA-LysM1 model these labelled positions are predicted at the protein surface (Figure 2.3).

The binding capacity of a LysM tandem towards BLPs and puri ed cell walls can also be measured by taking advantage of the intrinsic uorescence properties of the LysM tandem. The uorescence intensity became stable when $>$ 2.5 10^7 BLPs were added to 1.25 g of 5HW labelled W20 LysM tandem in solution, (Figure 2.6A). This result

showed that under the used conditions 1 μg of LysM tandem (LysM motif concentration of 1 μM) binds $\sim 2 \times 10^7$ BLPs. This result is in good congruence with a previously published report stating that 1 μg of AcmA-LysM domain is needed for saturated binding to 1.7×10^7 BLPs [71]. When the 5HW labelled W20 LysM tandem was titrated with PG the same fluorescence intensity change was obtained as for BLPs (Figure 2.6). The similar decrease in fluorescence intensity supports the view that LysM interact with the PG part of the cell wall. The saturation point was reached when 1.2 μg of PG was added, corresponding to a binding capacity of 1.2 μg of purified cell walls per 1 μg LysM tandem.

2.5 Discussion

Much progress has been made in understanding the physiological role of the LysM domains [55]. Still there is limited information available about how LysM domains interact with their ligand. To investigate the LysM structure - function relationship and the kinetics of the LysM - ligand interaction in more detail, an easy to use and sensitive methodology is needed to directly monitor the LysM - ligand interaction. In this work such a methodology is presented, based on the intrinsic Trp analogue fluorescence properties of LysM. A model of AcmA-LysM1 was generated to find residue positions which are close to the binding site and could be exchanged to a Trp analogue, allowing monitoring the ligand-binding event via fluorescence. In the AcmA-LysM1 model Asp11, as part of the highly conserved GDTL sequence, is located in the loop between β-strand 1 and α-helix 1 (Figure 2.3). It lies at the end of shallow groove on the surface of the domain. This region was proposed before in MltD-LysM as ligand-binding site [63]. Based on this hypothesis and the docking results, the Tyr at positions 5 and 20 and Gly at position 15 were substituted for Trp because they are positioned close to the putative substrate binding site. In initial experiments, LysM tandem proteins, labelled with Trp, were produced, isolated, and titrated with purified cell using an excitation wavelength of 295 nm. This induced a change in emission intensity of the W5, W15, W20, and W39 proteins of up to -16%, -13%, -25%, and +4%, respectively (data not shown). Thus, the engineered Trp residues near the putative binding site do report on the ligand-binding event. The high autofluorescence of BLPs, when excited at 295 nm, prevented a similar titration experiment. BLPs contain proteins and the autofluorescence of BLPs is much lower when excited at 305 or 310 nm. Replacing Trp by 7AW or 5HW in the tandem proteins enables monitoring the binding of BLPs to LysM when excited at 305 or 310 nm. The autofluorescence intensity at the highest BLP concentration used in this work (2.5×10^7 particles per mL) was more than 10-fold lower than the fluorescence intensity of the 7AW or 5HW-labelled LysM tandem protein at 0.5 μM. This demonstrates the potential of these analogues when a high Trp background is present in the solution [22, 95, 36].

An ELISA test showed that the introduction of Trp analogues at these 3 positions resulted in functional constructs although a lower binding affinity for BLPs and purified cell walls was measured, suggesting that these residues are involved in substrate binding. The fluorescence of these 3 constructs changed significantly upon ligand binding. In contrast, the fluorescence of W39 LysM tandem, in which the Trp is located at a distant position to the putative binding site, did not change notably upon substrate binding. This mutant showed a similar ligand binding affinity as the double Trp LysM tandem containing Trp at the wild-type position. Taking together, the selected residue positions Tyr5, Gly15, and Tyr20 in the AcmA-LysM1 model can be replaced by a Trp codon allowing efficient labelling with Trp analogues to detect ligand-binding events in a sensitive way.

The presented fluorescence approach allows the detection of low amounts of ligand, when 5HW-labelled W20 and the double-Trp LysM tandem proteins are used given that the fluorescence intensity of these two proteins was found to be the most sensitive for ligand binding. For example when 1.25 μg of LysM tandem was used, as low as 2×10^6 BLPs can be detected, as this amount of BLPs induced a fluorescence change of $\sim$10%. The same change in fluorescence is induced when 0.2 μg of purified cell walls is present in the solution.

The fluorescence of 7AW is known to be more sensitive for changes in the microenvironment than 5HW [78]. We found that the change in emission intensity of the two 5HW-labelled proteins upon ligand binding (Figure 2.5B and 2.5D) is larger than observed for the same proteins labelled with 7AW (Figure 2.5A and 2.5C). At the moment we have no proper explanation for this observation.

The method reported here can be used to address LysM related issues: (i) to discover other ligands besides the GlcNAc-MurNAc-Ala unit; (ii) to determine whether the affinity for LysM is affected by the length of the PG polymer and (iii) to determine the pre-steady state kinetics of the binding event. In addition, the approach presented in this work may find application in a biosensor for monitoring the presence of PG or bacterial cells in turbid solutions, including solutions with a high autofluorescence when excited $<$ 305 nm.

Acknowledgments

This work was supported by the nanotechnology network NanoNed. The authors are grateful to Biomade Technology Foundation for their support and making available their facilities to carry out part of the work.

2.6 Supplementary gures

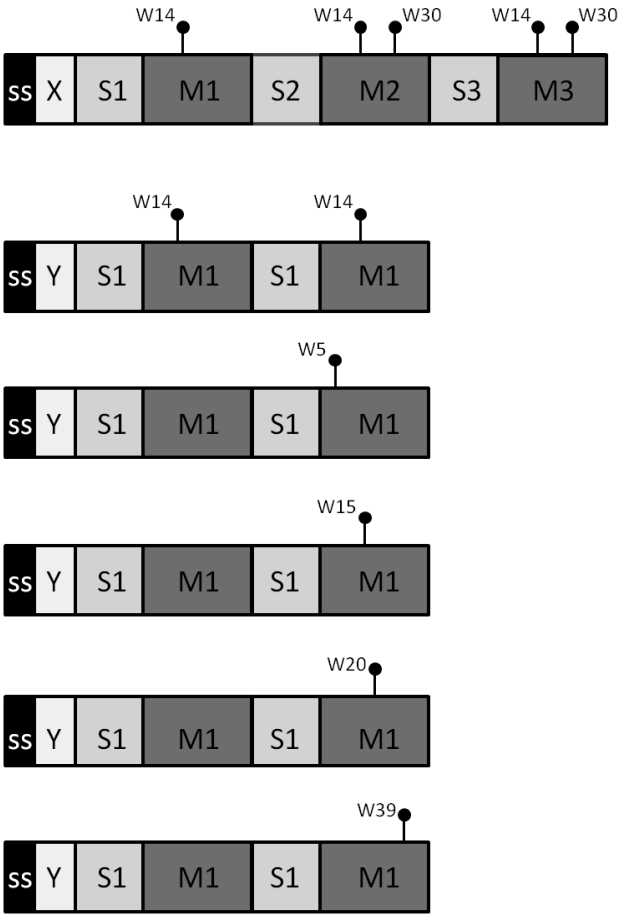

Figure 2.7: Schematic representation of proteins:(A) N-acetylglucosaminidase (AcmA); (B) wild type double Trp LysM tandem; (C) W5 LysM tandem; (D) W15 LysM tandem; (E) W20 LysM tandem and (F) W39 LysM tandem. X - catalytic part of the AcmA; Y - c-myc; S1-S3 - spacer sequences; M1-M3 - LysM motifs. The Trp positions in the proteins are indicated.

Chapter 3

An expression system for the efficient incorporation of an expanded set of tryptophan analogues

Dejan M. Petrović, Kees Leenhouts, Maarten L. van Roosmalen, Jaap Broos

Published in *Amino Acids*, 2013, Volume: 44, page: 1329-1336.

3.1 Abstract

Biosynthetic incorporation of tryptophan (Trp) analogues in recombinant proteins using an *E. coli* Trp auxotroph expression host is limited to analogues modified with a small substituent like a fluoro atom or a hydroxyl or amine group. We report here the efficient incorporation (> 89%) of chloro- and bromo- atoms-containing Trp analogues in alloproteins at high expression levels using a *Lactococcus lactis* Trp auxotroph strain. This result was only obtained after coexpression of the enzyme tryptophanyl-tRNA synthetase of *L. lactis* (lacTrpRS), an enzyme believed to show a more relaxed substrate specificity than TrpRS from *E. coli*. Chloro- and bromo-Trps are attractive intrinsic phosphorescence probes as these Trp analogues are much less sensitive than Trp for quenchers in the medium, like oxygen. Coexpression of lacTrpRS was also essential for the biosynthetic incorporation (94%) of the Trp analogue 5,6 difluoroTrp. This makes our expression system ideally suited to generate a set of methyl- and fluoro-substituted Trp analogue-containing alloproteins in high yield for investigating the involvement of the Trp residue in cation-π or π-π interactions. Taken together, the presented Trp auxotroph expression system features the most relaxed specificity for Trp analogue structures reported to date and gives a high alloprotein yield.

3.2 Introduction

Incorporation of non-canonical amino acids is an attractive strategy for introducing novel chemical and physical properties in recombinant proteins. For global replacement of an amino acid for its analogue in a recombinant protein an amino acid auxotroph expression strain is used, and the expression of alloproteins, proteins containing an unnatural amino acid, is relatively simple. A high incorporation efficiency of the amino acid analogue is often achieved together with a good alloprotein expression level [96, 97, 98, 99]. Only amino acid analogues which are structurally close to the natural amino acids can be incorporated in this way, a consequence of the high substrate specificity of the aminoacyl-tRNA synthetase (aaRS) enzymes. AaRS catalyses the activation of its cognate amino acid using ATP and its coupling to the corresponding tRNA, yielding aminoacyl-tRNA. In recent years, several developments to expand the set of non-canonical amino acids which can be incorporated under *in vivo* conditions, have been reported. Successful strategies include rational design of the amino acid binding pocket of aaRS, or coexpression of aaRS in the expression host [47, 53, 48, 49].

To date, a limited number of tryptophan (Trp) analogues have been biosynthetically incorporated in proteins, namely mono-substituted fluoroTrps, aminoTrps and hydroxyTrp analogues [100, 101, 102, 97]. Incorporating Trp analogues containing a bulkier substituent in proteins was not successful [103, 22] except in one study where a designed orthogonal aaRS/tRNA pair was introduced in *E. coli*, allowing incorporating 6-chloroTrp (6ClW) and 6-bromoTrp (6BrW), but not 5-bromoTrp (5BrW), at an amber codon position in the gene of the target protein [104]. This is an attractive strategy to label proteins [50]; however, development of an orthogonal aaRS/tRNA pair is not trivial and typically a low alloprotein yield is obtained.

Recently we reported the use of a *L. lactis* Trp auxotroph as host to incorporate Trp analogues, including 5-methylTrp (5MeW) [54], a Trp analogue not translated by *E. coli* [103]. This result suggests that the substrate specificity of *L. lactis* tryptophanyl-tRNA synthetase (lacTrpRS) is more relaxed than *E. coli* tryptophanyl-tRNA synthetase (ecoTrpRS).

In this report, we present an approach to increase the number of Trp analogues which can be incorporated efficiently by *L. lactis* (Figure 3.1). To achieve this, lacTrpRS was co-expressed together with the recombinant target protein. We show here that coexpression of lacTrpRS into the *L. lactis* Trp auxotroph results in efficient incorporation (89% - 97%) of all investigated Trp analogues in recombinant proteins together with a high expression levels.

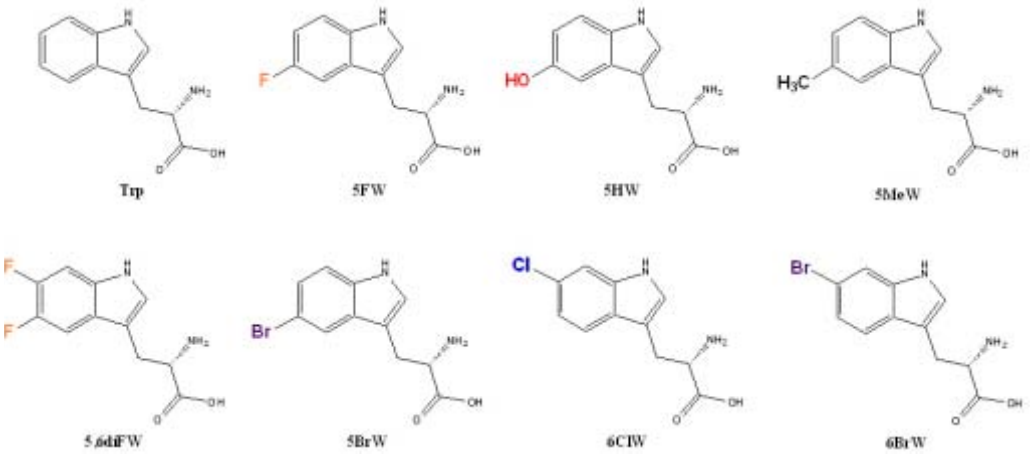

Figure 3.1: Structures of tryptophan and its analogues used in this study: Trp - tryptophan; 5FW - 5- uorotryptophan; 5HW - 5-hydroxytryptophan; 5MeW - 5-methyltryptophan; 5,6diFW - 5,6-di uorotryptophan; 5BrW - 5-bromotryptophan; 6ClW - 6-chlorotryptophan; 6BrW - 6-bromotryptophan

3.3 Materials and methods

3.3.1 General DNA techniques and transformation of *L. lactis*

Standard recombinant DNA techniques were performed as described previously [83] or as speci ed by the manufacturers. Enzymes and bu ers were purchased from BioLabs - New England or Roche. Nucleotide sequence analysis and DNA synthesis were performed by BaseClear (Leiden, The Netherlands).

The *trpRS* gene encoding tryptophanyl-tRNA synthetase was ampli ed from *L. lactis* MG1363 chromosomal DNA via PCR using pFU Taq DNA polymerase and the following primers: trpRS$_{fw}$ (5 -AAAGAGCTCAAAGGAGAAAAAAATGACAAAA CC) and trpRS$_{rev}$ (5 -AAACTGCAGAGGTGTCAAAACAATGAATTACC) containing SacI and PstI restriction sites, respectively. The ampli ed fragment was puri ed using a PCR puri cation kit (Qiagen) and subsequently cloned into the pMG36e expression vector [105], using SacI and PstI restriction enzymes and T4 DNA ligase, yielding plasmid pMG36e-trpRS.

Plasmid pPA295, containing the W20LysM tandem gene [106], was derived from a nisin inducible expression-secretion vector pNZ8048 [84], and electrotransformed into freshly prepared electrocompetent *L. lactis* PA1002 cells harboring the pMG36e-trpRS plasmid using a Bio-Rad Gene Pulser (Bio-Rad) [85].

3.3.2 Chemo-enzymatic synthesis and purification of tryptophan analogues

5-hydroxyTrp (5HW), 5MeW and 5BrW were from Sigma-Aldrich. 5-fluoroTrp (5FW), 5,6-difluoroTrp (5,6diFW), 6ClW and 6BrW were synthesized using a modified published procedure [107]. In brief, 17.5 mol acetic acid, 1.8 mmol acetic anhydride, 0.4 mmol of L-serine (Acros Organics) and 0.2 mmol of indole analogue, 5F-indole (Sigma-Aldrich), 5,6diF-indole (Biosynth), 6Cl-indole (Biosynth), or 6Br-indole (Biosynth), respectively, were mixed and the solution deaerated via purging with argon gas. This solution was incubated for 3 h at 73 °C. Subsequently, 10 ml of sodium-borate buffer, pH 8.0, containing 0.125 mM cobalt(II)-chloride was added to the reaction mixture, and the pH was adjusted to 8.0 with NaOH. Amano-acylase from *Aspergillus niger* (Sigma-Aldrich) was added at a concentration of 10 mg/ml, and the solution incubated for 48 h at 37 °C with shaking (250 rpm). The solution was centrifuged for 10 min at 5,400 × g and the supernatant was loaded in 2.5 ml portions on a PD-10 Desalting column (Amersham Bioscience), pre-equilibrated with 10 mM NaOH. Tryptophan analogues were eluted in 2 ml fractions from the column using 10 mM NaOH. Fractions with the highest A_{280}/A_{405} ratio were pooled and concentrated 8 times in a vacuum concentrator (Eppendorf).

The purity of the synthesized Trp analogues were determined via silica-gel thin-layer chromatography (TLC) with butanol:H_2O:acetic acid (4:1:1) as mobile phase. Visualization was done in iodine vapor [108].

3.3.3 *L. lactis* growth, protein expression and purification

Lactococcus lactis Trp auxotroph PA1002 [54], harboring the pPA295 and pMG36e-trpRS plasmids, was grown overnight at 30 °C in GM17 broth (M17 (Oxoid) supplemented with 0.5% (w/v) glucose) [86], 5 μg/ml of chloramphenicol and 75 μg/ml of erythromycin. Subsequently, 50 ml fresh GM17 medium with 5 μg/ml of chloramphenicol and 75 μg/ml of erythromycin was inoculated with this overnight culture (1:50) and growth at 30 °C was continued until an OD_{600} of 0.8. The cells were harvested by centrifugation at 5,400 × g for 10 min at 30 °C, washed three times with PBS at 30 °C, and resuspended in 50 ml CDM (chemically defined medium) [87] supplemented with 0,5% (w/v) glucose and 1 mM of all amino acids, except Trp. After a starvation period of 30 min at 30 °C, nisin, 1 mM Trp or Trp analogue was added, as described [54]. The cells were subsequently incubated for 18 h at 30 °C.

The LysM tandem protein is secreted by *L. lactis* and it is the most abundant protein in the culture supernatant. After centrifugation, the supernatant was loaded on an Amicon concentrator device (MWCO 3 kDa) and washed with phosphate buffered saline (PBS), pH 7.4. LysM alloprotein concentrations were determined by comparing the in-

tensity of the alloprotein bands with BSA as standard via an SDS-PAGE, gel stained with 0.05% Coomassie Brilliant Blue R-250 solution, using GelQuant.NET software provided by Biochemlabsolutions.

3.3.4 Mass spectrometry

20 μl aliquots of W20LysM tandem protein ($\approx$0.1 mg/ml) in PBS, pH 7.4 was exchanged to 100 mM ammonium bicarbonate buffer using an Amicon concentrator (MWCO 3 kDa). 2 μl of a porcine trypsin (Promega) stock solution (55 μg/ml) was added and the sample was incubated for 3 h at 37 °C. 0.75 μl was spotted on a MALDI (matrix-assisted laser-desorption ionization) target and mixed immediately with an equal volume of 10 mg/ml α-cyano-4-hydroxycinnamate (LaserBio Labs) in 50% acetonitrile / 0.1% (v/v) trifluoroacetic acid. Spots were recorded on a Voyager DE-PRO MALDI-TOF (time of flight) instrument (Applied Biosystems). Spectra were calibrated externally with standard peptides. Noise filter (correlation factor of 0.9) and Gaussian smoothing (filter width of 19 points) were applied to all spectra using Data Explorer (TM) software (Applied Biosystems). The Trp analogue incorporation efficiency was calculated by measuring the peak areas of the Trp analogue containing peptide and the Trp containing peptide.

3.3.5 Fluorescence

Steady-state fluorescence spectra were recorded with a Fluorolog-3.2.2 fluorimeter (Jobin-Yvon, Edison, NJ, USA). A protein concentration of approximately 0.1 mg/ml was used. W20LysM tandem containing 5FW, 5HW and 5MeW, were excited at both 295 nm and 305 nm. Excitation slits were set up at 0.5 nm, emission slits were set at 5.00 nm and 3 $\times$ 3 mm quartz cuvettes were used. Fluorescence emission was measured from 320 nm to 450 nm at 23 °C. Spectra were corrected for the PBS buffer emission.

3.4 Results

3.4.1 Cloning and overexpression of lacTrpRS

The nucleotide sequence of the genome of the lactic bacterium *L. lactis* subsp. cremoris MG1363 is known (NCBI, GenBank: AM406671.1 http://www.ncbi.nlm.nih.gov/nuccore/AM406671) [109] and we identified the *trpRS* gene in the locus llmg_0079. Using PCR, a fragment of 1075 base pairs (bp) comprising the *trpRS* nucleotide sequence (1025 bp) and a putative ribosome-binding site was amplified and cloned into the pMG36e plasmid [105] behind the strong constitutive promoter P32 [110]. The newly constructed plasmid, pMG36e-trpRS, was transformed into the *L. lactis* PA1002 Trp auxotroph strain

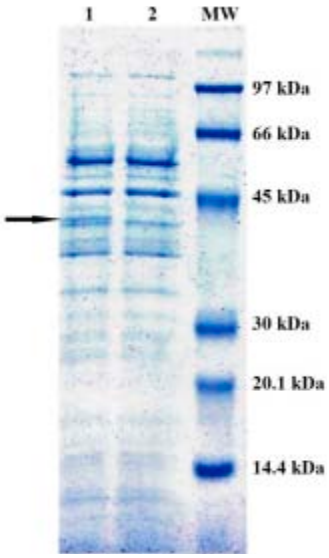

Figure 3.2: Expression of lacTrpRS recombinant protein in *L. lactis* PA1002, visualized via a 12.5% SDS-PAGE Lane 1: *L. lactis* PA1002 harboring lacTrpRS encoding plasmid (black arrow indicate lacTrpRS band). Lane 2: *L. lactis* PA1002 harboring empty pMG36e plasmid

[54].

SDS-PAGE analysis of protein extracts of these cells harvested at OD_{600} $\gg$0.7 revealed the presence of a protein band at approximately 38 kDa (theoretical mass of lacTrpRS is 37963 Da). This band was not visible in a control experiment (Figure 3.2). This experiment demonstrated that lacTrpRS enzyme is well overexpressed in *L. lactis*, before the induction of the target protein is initiated.

3.4.2 Biosynthetic incorporation of Trp analogues into the W20LysM tandem protein

The *L. lactis* Trp auxotroph strain PA1002, harboring plasmid pMG36e-trpRS, was transformed with the plasmid encoding the single-Trp-containing target protein, W20LysM tandem [106]. The W20LysM tandem and the lacTrpRS containing plasmids comprise different promoters, P32 - constitutive promoter [105] and PnisA - nisin inducible promoter [111], respectively, and di erent selection markers, the genes for chloramphenicol and erythromycin resistance, respectively. Expression of the W20LysM tandem protein was performed in CDM supplemented with 1 mM Trp, or Trp analogue. Excellent expression levels of W20LysM tandem alloproteins were observed in all cultures (25 - 50 mg per 1 l of culture). Only in the presence of 5BrW or 6BrW slightly lower expression levels were observed (Figure 3.3). The high yield of alloproteins containing 5HW, 5,6diFW, 6ClW, 5BrW and 6BrW is due to the coexpression of lacTrpRS. When *L. lactis* PA1002 contains only W20LysM tandem-containing plasmid very low or no detectable expression of

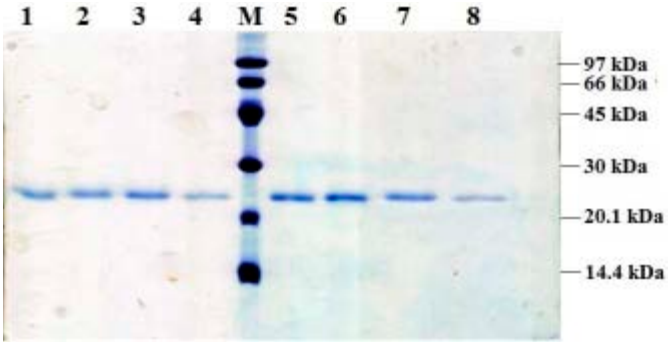

Figure 3.3: SDS-PAGE of culture supernatants after overnight expression of W20LysM tandem in the presence of Trp or a Trp analogue. W20 LysM tandem expressed in the presence of: Lane 1: Trp; Lane 2: 5FW; Lane 3: 5HW; Lane 4: 5BrW; Lane 5: 5MeW; Lane 6: 5,6diFW; Lane 7: 6ClW; Lane 8: 6BrW

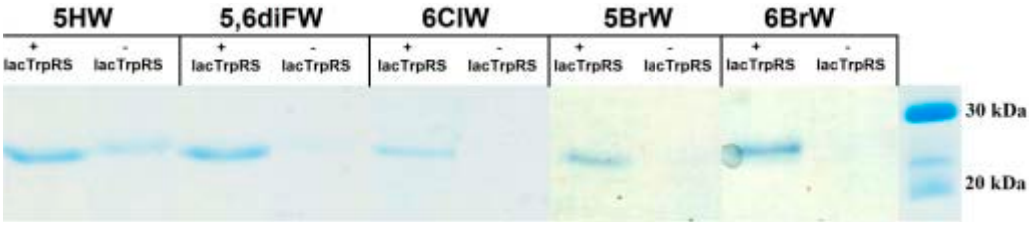

Figure 3.4: SDS-PAGE of culture supernatants of *L. lactis* coexpressing lacTrpRS [+] or without coexpressing lacTrpRS [-]. Samples were collected after overnight expression of W20LysM tandem in the presence of 5HW, 5,6diFW, 6ClW, 5BrW or 6BrW, respectively. MW is the molecular mass standard.

W20LysM was observed (Figure 3.4). For the 5FW- and 5MeW- containing W20LysM tandem expression levels were found only minimally dependent on coexpression of lacTrpRS (data not shown).

The incorporation e ciency of each Trp analogue in the target protein was established by MALDI-TOF mass spectrometry. For W20LysM tandem expressed in CDM supplemented with Trp, a tryptic peptide with a mass of 1629.67 Da was detected. This intense peak was absent or its intensity strongly reduced for W20LysM tandem expressed in the presence of a Trp analogue. In the mass spectra of these samples a new peak was present corresponding to the mass of the Trp analogue-containing peptide (Figure 3.5). Very high incorporation e ciencies (94%) were found for 5FW, 5HW, 5MeW and 5,6diFW, while for the other Trp analogues the incorporation e ciency was 90% (Table 1).

W20LysM tandem alloproteins containing 5FW, 5HW and 5MeW show a comparable uorescence quantum yield (Q) as W20LysM tandem containing Trp. The identical shape of the emission spectra, when excited at 295 nm or 305 nm, supports the view that

Trp analog	% incorporation
5FW	98±1%
5HW	95±1%
5BrW	90±2%
5MeW	95±1%
5,6diFW	94±2%
6ClW	91±2%
6BrW	89±3%

Table 3.1: Trp analogue incorporation efficiency into W20 LysM tandem protein.

the presence of Trp in these three protein samples is very low (Figure 3.6). The fluorescence Q of W20LysM tandem proteins containing 5,6diFW, 5BrW, 6ClW and 6BrW, respectively, is very low, < 0.01 (data not shown). Such a low fluorescence Q does not allow accurate comparison of emission spectra of the proteins when excited at 295 nm and 305 nm wavelengths, respectively.

3.5 Discussion

In this work we report an efficient strategy to incorporate Trp analogues including those not biosynthetically introduced in proteins before, with high incorporation efficiency and resulting in a high alloprotein yields. The single Trp-containing protein, W20LysM tandem, was used as target protein for the incorporation of Trp analogues. W20LysM tandem is a small 20 kDa protein and a 3D model of this protein suggests the Trp residue is at a surface-exposed position [106]. By choosing a surface exposed Trp position instead of a buried position minimizes the chance that its replacement with a bulky Trp analogue (e.g. 5BrW and 6BrW) compromises the folding and stability of the alloprotein.

Initial studies with 5BrW using the *L. lactis* Trp auxotroph PA1002 as expression host suggested that this analogue can be incorporated by *L. lactis*, as a very low amount of alloprotein was obtained. Cloning of the lacTrpRS behind the constitutive P32 promoter [105] and its coexpression together with the target protein resulted in large increase in the expression levels of alloproteins containing 5,6diFW, 6ClW, 5BrW and 6BrW, respectively. Expression levels were approximately equal to those obtained with Trp in the medium (∼50 mg/l); except that the alloproteins containing 5BrW and 6BrW expression levels were ∼50% lower. 5HW can also be incorporated without lacTrpRS coexpression, however a lower alloprotein yield (Figure 3.4) and a lower incorporation efficiency (89% versus 95%) are observed [54]. Similarly, the 5MeW incorporation efficiency increase from 92% to 94% when lacTrpRS was coexpressed.

The new alloproteins, which can now be produced relatively easily, offer novel op-

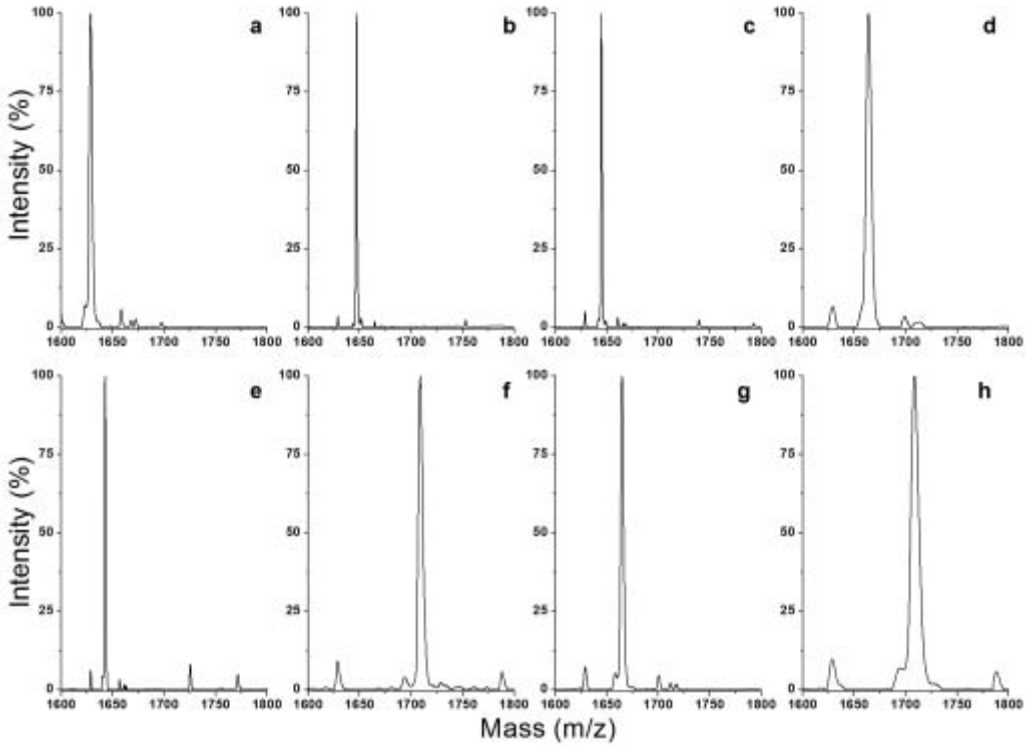

Figure 3.5: MALDI-TOF spectra of tryptic peptide of W20 LysM containing Trp or a Trp analogue. The mass region of the WGISVAQIQSANNLK peptide is shown. The peak of protonated peptide containing Trp (a), 5FW (b), 5HW (c), 5,6diFW (d), 5MethylW (e), 5BrW (f), 6ClW (g) and 6BrW (h), respectively, are shown.

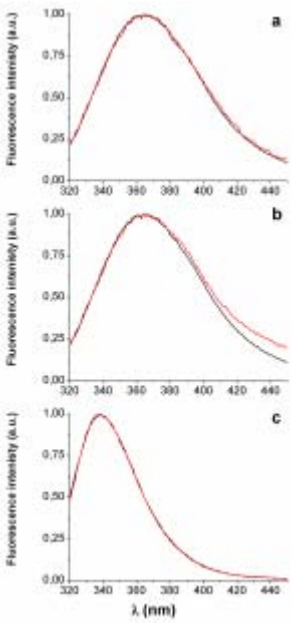

Figure 3.6: Emission spectra of W20LysM tandem alloproteins excited at 295 and 305 nm, respectively. Red line - emission spectrum of W20LysM tandem excited at 295 nm, black line - emission spectrum of W20LysM tandem excited at 305 nm; (a) 5HW; (b) 5FW; (c) 5MeW containing W20LysM tandem. Spectra were normalized.

portunities in protein structure and function studies. For example, evaluation of a set of alloproteins containing a Trp with electron-donating (methyl) or withdrawing (fluoro) substituents in the indole moiety offer a powerful means to study the role of a Trp residue in cation-π or π-π interactions [112]. So far, alloproteins used in such studies were produced in very low amounts via an *in vitro* methodology using *Xenopus laevis* oocytes as expression system. The chloro- and bromo substituted Trp analogues offer interesting opportunities as intrinsic phosphorescence probes. Trp phosphorescence spectroscopy is one of the most sensitive methodologies known to probe local viscosity in a protein and is also ideally suited to investigate if the protein is present in different conformational states [113, 114]. Widespread use of Trp phosphorescence is limited by the extreme sensitivity of the triplet state to quenchers, like oxygen [115]. For reliable measurements, the quencher concentrations in the buffer need to be reduced to the sub-nM concentration range. The high sensitivity is a result of the very long intrinsic triplet lifetime (6.5 s) of Trp [115], giving quenchers "ample time" to deactivate the triplet state. Chloro or bromo substitution of Trp strongly reduces the intrinsic triplet lifetime [116], making it 1 - 3 orders of magnitude less sensitive for quenchers like oxygen. Moreover, these substituents enhance the intersystem crossing rate from the singlet to the triplet state, thus suppressing fluorescence and increasing the phosphorescence intensity. We are currently investigating the spectroscopic properties of the various alloproteins via phosphorescence methodologies.

In summary, a versatile Trp analogue expression system was developed in *L. lactis*,

allowing the efficient biosynthetic incorporation of Trp analogues in proteins not reported before together with a high alloprotein yield.

Acknowledgments

This work was supported by the nanotechnology network NanoNed. The authors are grateful to Biomade Technology Foundation for their support and making available their facilities to carry out part of the work.

Chapter 4

Emitting state of 5-hydroxyindole, 5-hydroxytryptophan and 5-hydroxytryptophan incorporated in proteins

Dejan M. Petrović, Ben H. Hesp, and Jaap Broos

Published in *J. Phys. Chem. B*, 2013, Volume: 117, page: 10792-10797.

4.1 Abstract

5-Hydroxy-L-tryptophan (5HW) has been biosynthetically incorporated in many proteins to facilitate their characterization using fluorescence spectroscopy. An attractive feature of this tryptophan analogue is its absorbance at 310-320 nm, allowing its specific excitation in a Trp background. The red-shift in absorbance upon introduction of a hydroxyl group at the 5-position of Trp or indole was found to be due to a lowering of the ^1L_b transition energy. It was therefore believed that 5HW only features ^1L_b emission while the ^1L_a state is typically the emitting state for Trp. Recently, calculations for 5-hydroxyindole (5HI) in water revealed that the ^1L_a is the emitting state, and the same was predicted for 5HW incorporated in proteins. To clarify which state emits in 5HI and 5HW, we present here excitation anisotropy spectra of these probes and of four proteins labelled with 5HW at a surface exposed position. Our data clearly show that ^1L_b is the emitting state of 5HI, 5HW and of 5HW in three of the proteins investigated. For one protein mixed emission was observed, and the decay kinetics were found strongly dependent on the emission wavelength. This work provides the first experimental evidence that ^1L_a can be the emitting state for this Trp analogue incorporated in a protein.

4.2 Introduction

Tryptophan (Trp) fluorescence spectroscopy is widely used to study protein structure, dynamics and function [3]. Most information can be extracted when a single-tryptophan-containing protein is studied. Experimental observables include the quantum yield, spectral energy of the emission, and anisotropy. These observables are related to return of the excited electron from the lowest electronically excited state of the fluorophore to the ground state. Trp and Trp analogues have four singlet valence π - π^* electronic excited states, the lower energy ^1L_a and ^1L_b states and the higher energy ^1B_a and ^1B_a states [17]. Only the two ^1L states play a role in Trp and Trp analogue fluorescence and their absorption spectra extensively overlap. The excited-state conversion between the ^1L_a and ^1L_b states is known to be extremely fast [117], and the transition dipole moments of the ^1L_a and ^1L_b states of indole are nearly perpendicular to each other [118]. In the gas phase the ^1L_b state of indole is 0.3 eV lower in energy than the ^1L_a state [119]. In most media, ^1L_a becomes the lowest excited state, a result of the more efficient stabilization of the large ^1L_a dipole moment (5 - 6 D) via solute interactions compared to the smaller dipole moment of the ^1L_b state ($\approx$2 D) [120, 119]. ^1L_b is the emitting state only for indole in the gas phase or when dissolved in perfluorohexane [18, 119]. Moreover, three single-Trp-containing mutants of transhydrogenase domain 1 emit from both the ^1L_b and ^1L_a state [20, 19]. In these proteins, the Trp is embedded in a very rigid and apolar protein core.

Substitution of a hydroxyl group at the 5-position of indole results in a red-shift of the absorption spectrum. The absorption of the red-extended shoulder of 5-hydroxytryptamine (serotonin) is due to ^1L_b absorption, and ^1L_b is the emitting state [121]. Lami reported the same for 5-hydroxyindole (5HI) [122, 22]. Thus introduction of a hydroxyl group at the 5-position increases the ^1L_a - ^1L_b gap [32] and in most publications it is assumed that ^1L_b is the emitting state in 5-hydroxytryptophan (5HW) and 5HI [123, 124, 125, 30]. Dipole moments of 2.14 D and 2.04 D were calculated for the ground and ^1L_b states, respectively, of 5HI [126] and in accordance with this, a small variation in emission maximum (λ^{max}) of 5HI in different solvents (cyclohexane λ^{max} = 322 nm; water λ^{max} = 331 nm) is observed compared to the ^1L_a emitting indole (cyclohexane λ^{max} = 298 nm; water λ^{max} = 342 nm) [122, 22]. Recent theoretical studies challenged the generally accepted idea that free 5HI dissolved in water, or 5HW incorporated into proteins, show emission from ^1L_b [126, 127]. H-bonding to the 5-hydroxy group was found to decrease the ^1L_a - ^1L_b gap with ^1L_a becoming the emitting state when either one water molecule makes a single long H-bond with the hydroxy group or if two water molecules make H-bonds with the hydroxy group. An experimental study to investigate the fluorescing state of 5HI, 5HW and 5HW-containing proteins has not been presented. Excitation anisotropy spectra of indole and its derivatives can accurately establish the emitting state and we used this approach recently to establish the emitting state of the most blue-emitting single-Trp containing

proteins known, azurin, transhydrogenase domain 1 and mutants of these proteins [20, 19]. Here we use the same approach to establish the emitting state of 5HI, 5HW and 5HW incorporated in four proteins at a single position. ^1L_b was found to be the emitting state for free 5HI and 5HW and data are presented showing the protein matrix can promote the ^1L_a state to become emitting, as dual emitting was observed for 5HW in one of the proteins investigated.

4.3 Materials and methods

4.3.1 Materials

5-Hydroxy-L-tryptophan (5HW) was purchased from Sigma-Aldrich, 5-hydroxyindole was from TCI, and glycerol (spectroscopic grade) was from Merck.

LysM tandem proteins. Biosynthetic incorporation of 5HW in single Trp mutants of the LysM tandem protein and its purification were done as described in detail before [128]. This protocol results in a 95% incorporation efficiency of 5HW in LysM tandem protein.

4.3.2 Spectroscopy

Fluorescence spectra were recorded with a Fluorolog 3-22 fluorospectrometer (Jobin Yvon) equipped with Glan-Thompson polarisers in L-format. Excitation slit widths of 3 nm were used for 5HW and 5HI and 5 nm for LysM tandem protein experiments. Band passes of 3 nm were used for 5HW and 5HI and 5 nm for LysM tandem protein experiments. The emission band passes were at 5 nm. Steady state excitation and emission spectra were recorded with emission monitored at 340 nm and excitation at 295 nm, respectively, and the spectra were corrected for instrument response. Low-temperature spectra were recorded with a quartz Dewar set up and a quartz tube (r = 2.5 mm). Solid CO_2 was added to 99 % ethanol and used to cool the sample to -50 °C. Glass samples were prepared by mixing 5HI, 5HW, or 5HW-containing LysM tandem protein in phosphate buffered saline (PBS) pH 7.4 with glycerol (30:70 (v/v)). The final concentration of 5HW, 5HI and LysM tandem containing 5HW were 6-30 μM.

Time resolved emission detection was performed by a streak camera system equipped with a spectrograph (Hamamatsu C5680, Chromex 250 mm). Excitation was at 300 nm and the time resolution was 200 ps. Data was analysed using a standard Levenberg-Marquardt fitting method [129].

4.4 Results

We started our investigation by collecting data for free 5HW, 5HI, and 5HW-labelled single-Trp W20LysM tandem protein. This protein of 20 kDa shows a high binding affinity for peptidoglycan and a Trp codon was introduced at residue position 20 allowing monitoring peptidoglycan binding via Trp analogue fluorescence spectroscopy [106].

The λ^{max} values of free 5HI, 5HW and the alloprotein in a glycerol glass at -50 °C are at 328 nm, 335 nm, and 336 nm, respectively, and anisotropy excitation spectra were recorded by collecting emission at 320 nm, 340 nm, and 360 nm, respectively (Figure 4.1 and Figure 4.5).

For free 5HW all three recorded spectra are similar in shape; thus the fluorescence of 5HW at the 3 wavelengths is the same. In line with this observation, r_0 was found essentially independent of the emission wavelength (Figure 4.2A). The gradual increase of r_0 with increasing excitation wavelength (λ_{ex}) is expected for ^1L_b as emitting state as it dominates the absorbance spectrum at the red-edge of 5HW. The equation

$$r_{0\lambda} = f_a(\lambda)r_{0a} + f_b(\lambda)r_{0b}$$

is needed for resolving the individual ^1L_a and ^1L_b spectra of 5HW. $r_{0\lambda}$ is the observed anisotropy at wavelength λ and r_{0a} and r_{0b} are the limiting anisotropies of the ^1L_a and ^1L_b states at wavelength λ, respectively. $f_a(\lambda)$ and $f_b(\lambda)$ are the fractional contributions of the ^1L_a and ^1L_b transition states at wavelength λ with $f_a(\lambda) + f_b(\lambda) = 1$ [3]. As red edge excitation of 5HW only yields ^1L_b emission ($f_a(\lambda) = 0$)[122, 123], r_0=r_{0b}. From figure 4.1A it follows that $r_0 = r_{0b} = 0.35$, a value significantly higher than reported before for 5HW ($r_0 = 0.25$) [100], but the same value as obtained for 5-methoxytryptophan [130]. The limiting anisotropy for ^1L_a can be calculated using equation:

$$r_{0a} = r_0 \frac{3cos^2\beta - 1}{2}$$

with $r_0 = 0.35$ and β the angle in space between the ^1L_a and ^1L_b transient absorption dipole moments [3]. For $\beta = 0°$, 45°, and 90°, this yields r_{0A} values of 0.35, 0.0875 and -0.175, respectively. The negative r_0 values presented in figure 4.1A at $\lambda_{ex} < 285$ nm indicate that a large β value exist in 5HW. At $\lambda_{ex} < 285$ nm, the excitation spectrum of 5HW is dominated by ^1L_a and its excitation is followed by rapid transfer to the lower lying ^1L_b emitting state. The contributions of ^1L_a and ^1L_b to the excitation spectrum of 5HW at wavelength λ, can be calculated using equations:

$$I_a(\lambda) = f_a(\lambda) \cdot I(\lambda)$$

$$I_b(\lambda) = f_b(\lambda) \cdot I(\lambda)$$

where $I_a(\lambda)$ and $I_b(\lambda)$ are the intensities of the excitation spectra of ^1L_a and ^1L_b, respectively, at wavelength λ. β values between 0° to 66° result in negative ^1L_a amplitudes (data not shown); thus, β values are too small as negative excitation amplitudes are not acceptable. β values between 67° - 90° give subspectra with positive amplitudes and these spectra are presented in figure 4.6B for $\beta = 90°$ and figure 4.6A for $\beta = 67°$. The spectra are very similar to the two published subspectra of 5-methoxytryptophan ($\beta = 90°$) [130]. Both ^1L_a spectra peak at 270 ±3 nm and do extend far into the red-edge of the 5HW and 5-methoxytryptophan excitation spectra, respectively. The two ^1L_b spectra show the lowest transition energies in these two Trp analogues. Analysis of the 5HI data in a similar way ($r_0 = 0.34$, $\beta = 90°$) gave ^1L_a and ^1L_b spectra alike the spectra obtained for 5HW and with ^1L_b showing the lowest transition energy (Figure 4.3B). Only β values of 66° - 90° gave subspectra with positive amplitudes (Figure 4.7).

In 5HW-labelled W20LysM tandem protein, 5HW at residue position 20 is predicted to be surface exposed [106] and anisotropy excitation spectra of this protein, recorded using the same condition as for 5HW and 5HI, are shown in figure 4.1B. The three recorded spectra differ in shape with only the spectrum collected at 360 nm showing a similar shape as for free 5HW and 5HI. For the spectrum collected at 320 nm, r_0 at $\lambda_{ex} < 285$ nm is much higher than that for free 5HW but r_0 drops sharply at $\lambda_{ex} > 285$ nm. The relatively high $f_a(\lambda) < 285$ nm, together with a high r_0 in this part of the spectrum is in agreement with ^1L_a emission collected at 320 nm. The strong increase in r_0 at $\lambda_{ex} > 292$ nm together with an increase in $f_b(\lambda)$ shows ^1L_b emission is also occurring at 320 nm. Thus 5HW-labelled W20LysM tandem shows a mixed emission at 320 nm. For the excitation anisotropy spectrum collected at $\lambda_{em} = 340$ nm, the contribution of ^1L_a emission is less than at 320 nm as only a small dip in r_0 is observed at $\lambda_{ex} = 285$ - 292 nm. The excitation anisotropy spectrum collected at 360 nm does not show evidence for ^1L_a emission occurring in this part of the emission spectrum. The dependence of r_0 on the emission wavelength at 3 of the 4 different λ_{ex} investigated (Figure 4.2B) is in accordance with mixed emission for this sample. For $\lambda_{ex} = 305$ nm, r_0 is minimally dependent on the emission wavelength, a result consistent with only ^1L_b emission is generated at this wavelength. Taken together, the anisotropy data of 5HW-labelled W20LysM tandem provide for the first time experimental evidence for mixed emission of this Trp analogue.

^1L_a emission is centred at the blue part of the emission spectrum of W20LysM tandem protein, while at the red part of the emission spectrum only ^1L_b emission is observed. The calculated excited dipole moments of the ^1L_a and ^1L_b states of 5HI are 6.51 D and 2.04 D, respectively [126]. As the emission was collected in a glass, full spectral relaxation is not possible under these conditions, unlike in fluid medium. This explains why the ^1L_a

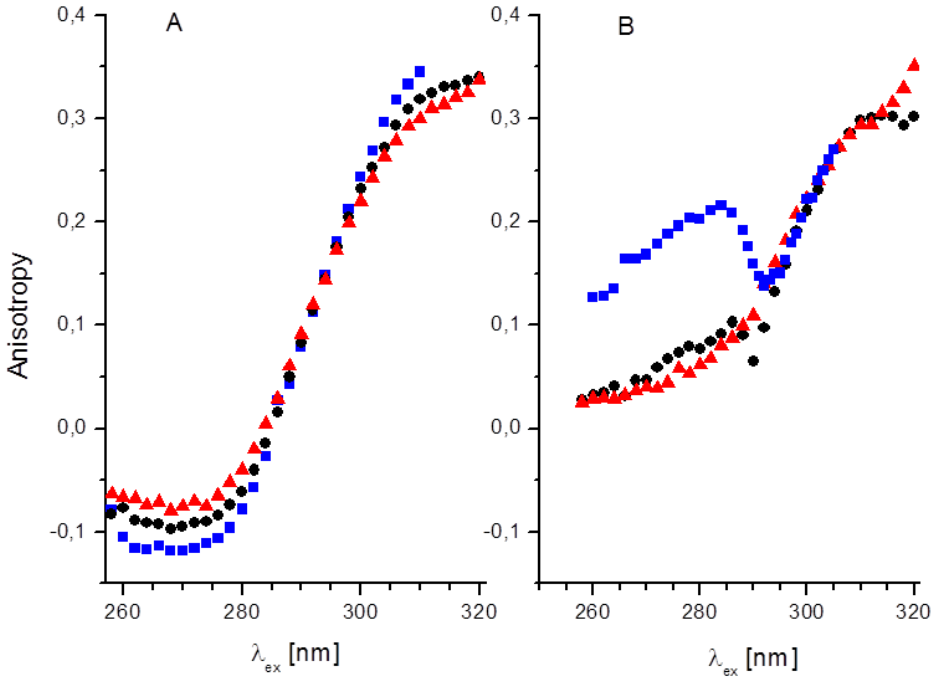

Figure 4.1: Anisotropy excitation spectra of free 5HW (A) and 5HW containing W20 LysM tandem (B) in a glycerol glass at -50 °C. Emission was recorded at 320 nm (blue), 340 nm (black) and 360 nm (red).

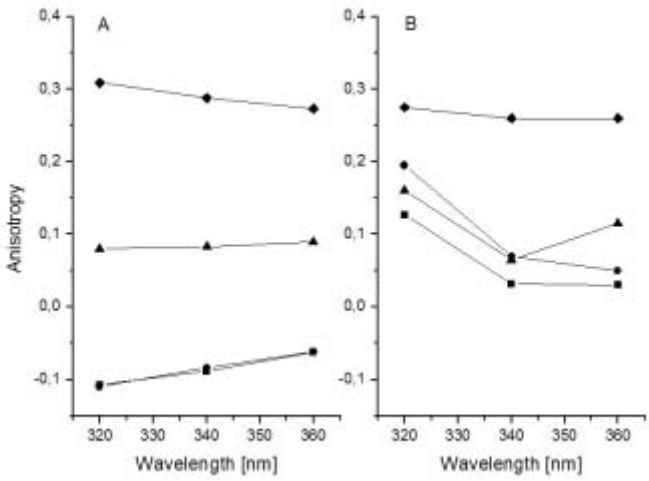

Figure 4.2: Emission wavelength dependence of the anisotropy of free 5HW (A) and 5HW containing W20LysM tandem (B) in a glycerol glass at -50 °C. Excitation wavelengths of 260 nm (square), 275 nm (circle), 290 nm (triangle), 305 nm (diamond) were used.

transition, centred at the blue part of the absorbance spectrum of 5HW, is also observed at the blue part of the emission spectrum.

4.4.1 Time-resolved fluorescence analysis of 5HW- and 5HW-labelled W20LysM tandem protein

5HW dissolved in water at pH 7 shows a single-exponential fluorescence decay [22], but when incorporated into proteins it typically shows two or three lifetimes, with values varying from less than 0.1 ns to 5 ns [37].

A streak camera was used to study the fluorescence decay kinetics of free 5HW and 5HW containing W20LysM tandem protein at emission wavelengths 320 nm, 340 nm, and 360 nm and the results are presented in table 1 and in figure 4.8.

For free 5HW at all three emission wavelengths the decay shows a single lifetime of 3.5 ns, a result congruent with previous reports [30, 31, 131]. The decay of 5HW containing W20LysM tandem protein is best described by two exponentials, and the decay times are dependent on the emission wavelength (Table 1). The average lifetime, with individual lifetime contributions between 0.5 ns and 3.5 ns, increases with changing the emission wavelength from the blue to the red part of the spectrum. At 360 nm, the 3.5 ns lifetime dominates the decay, but 35 % of the decay amplitude corresponds with a lifetime of 1.1 ns.

Sample	λ emission (nm)	τ_1 (ns)	α_1 (%)	τ_2 (ns)	α_2 (%)	χ^2
5HW	320	3.517	100	—	—	0.938
5HW	340	3.493	100	—	—	1.09
5HW	360	3.504	100	—	—	1.138
5HW-W20LysM	320	0.526	29	2.982	71	0.965
5HW-W20LysM	340	1.036	26	3.12	74	0.998
5HW-W20LysM	360	1.099	35	3.50	65	1.135

Table 4.1: Fluorescence decay parameters of free 5HW and 5HW containing W20 LysM tandem.

This shorter lifetime could be due to ^1L_a emission, appearing at this wavelength because the data were collected at fluid medium, shifting the ^1L_a emission to red wavelengths compared to the glass conditions presented in figure 4.2. However this short lifetime can also be a result of ^1L_b emission of a W20LysM tandem protein fraction in a quenched state. Overall, the strong dependence of the average lifetime on the emission wavelength is in agreement with mixed emission in 5HW labelled LysM proteins.

4.4.2 Emitting state of 5HW in three other single-Trp mutants of LysM tandem protein

5HW was also biosynthetically incorporated at positions 5, 15, and 39, respectively, of three other single Trp containing LysM tandem proteins. Like residue position 20, these three positions are at the protein surface [106]. Excitation anisotropy spectra of these three proteins, collected at emission wavelengths 320 nm, 340 nm, and 360 nm, are presented in figure 4.4. Following the same interpretation as presented above for 5HW, 5HI, and W20LysM tandem protein, all spectra presented in figure 4.4 are typical for only ^1L_b being the emitting state at the three investigated emission wavelengths.

4.5 Discussion

In this work we identified the emitting state of 5HI and 5HW, and of 5HW introduced in four mutants of the LysM tandem protein. The recorded excitation anisotropy spectra of these samples show that ^1L_b is the emitting state in 5HI, 5HW, and in 3 of the 4 proteins investigated. For the W20LysM tandem protein, mixed emission was observed

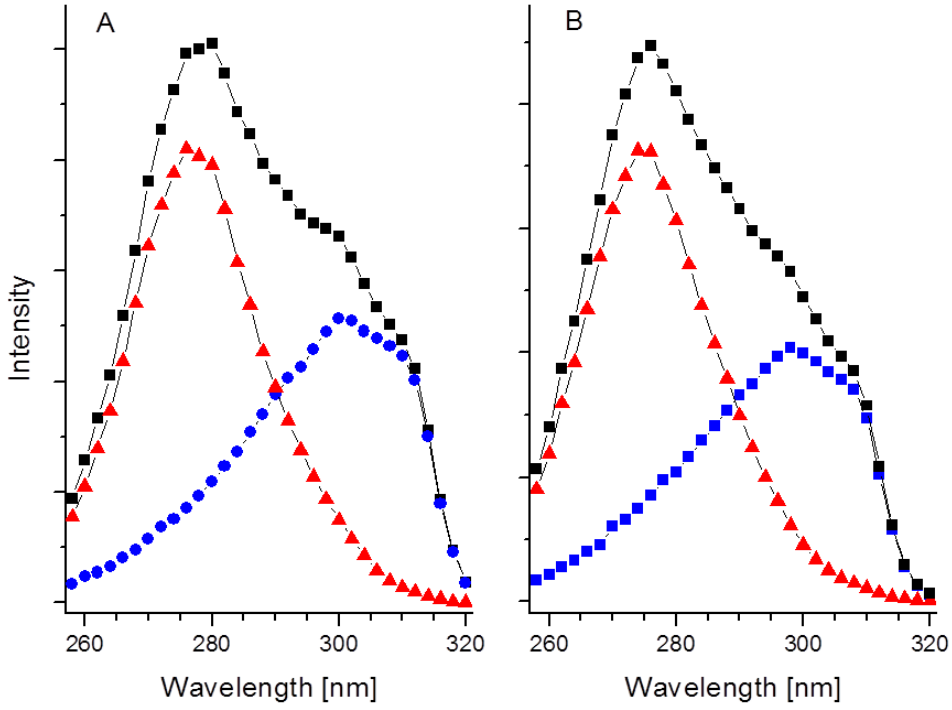

Figure 4.3: Fluorescence excitation spectra (square) of free 5HW (A) and 5HI (B) in a glycerol glass at -50 °C and their resolved ^1L_a (triangle) and ^1L_b (circle)spectra for $\beta = 90°$.

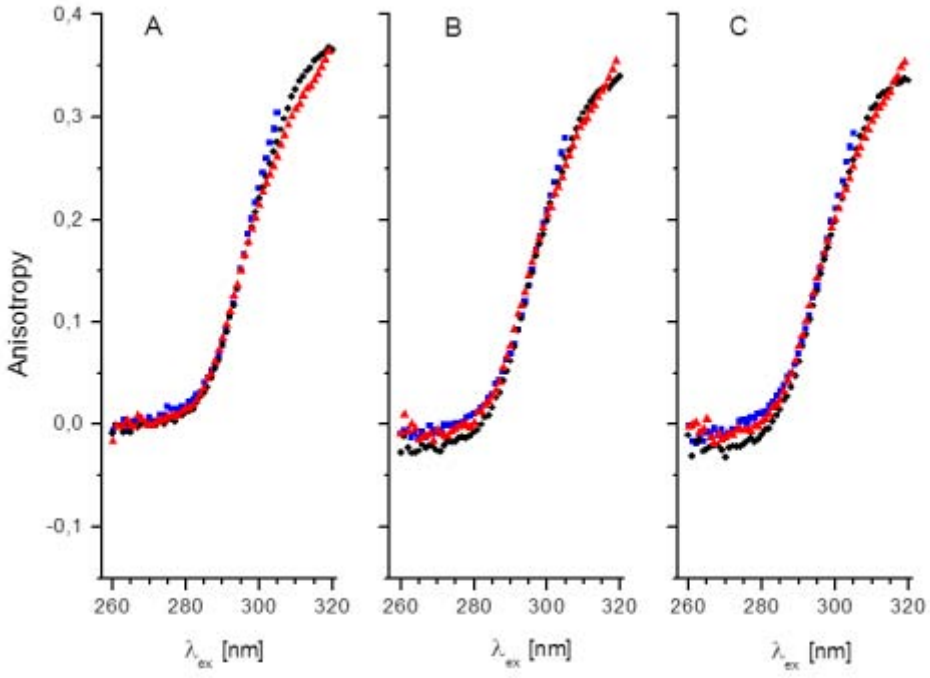

Figure 4.4: Anisotropy excitation spectra of 5HW containing proteins W5LysM tandem (A), W15LysM tandem (B) and W39LysM tandem (C), respectively, in a glycerol glass at -50 °C. Emission was recorded at 320 nm (square), 340 nm (circle) and 360 nm (triangle).

and in accordance with this, the fluorescence decay kinetics of this sample was found to be emission wavelength dependent. This work was motivated by disparate views in the literature on the emitting state of free 5HW and of 5HW-containing proteins. For approximately 20 years, 5HW has been biosynthetically incorporation into proteins, and its fluorescence has been employed to study protein structure [30, 31]. 5HW is known as an attractive, intrinsic optical probe of proteins, because of its red-shifted absorbance spectrum, compared to Trp, allowing its specific excitation at 310-320 nm. The high r_0 upon excitation at these wavelengths makes 5HW ideally suitable for anisotropy studies [30, 31]. Based on several studies [122, 32] it was accepted that in 5HW and 5HI, ^1L_b is the emitting state, while ^1L_a is typically the emitting state in Trp and most other Trp analogues characterized to date. However, Hirst and coworkers recently reported the ^1L_a state of 5HI in aqueous solution is the emitting state [126]. In this work, 10 ps snapshots of MD simulations of 5HI in water at 300 K were used in TDDFT calculations to generate the ^1L_a and ^1L_b absorption spectra of 5HI, and these spectra were compared with the experimental absorption spectrum. The calculated ^1L_b spectrum peaks at 297 nm - the same position as in the absorption spectrum (298 nm) [126]. The ^1L_b spectrum of 5HI, resolved from polarization experiments, also peaks at 298 nm (Figure 4.3B). The calculated ^1L_a spectrum shows a peak at 286 nm, while the experimental peak is at 274 nm [126]. Also the resolved ^1L_a spectrum in figure 4.3B peaks at 274 nm. Thus the calculations yielded an ^1L_a spectral peak at much lower energy than given by the available experimental data. This likely explains why also the ^1L_a origin of the 5HI spectrum was found at lower energy than the ^1L_b origin, leading to the conclusion that ^1L_a is the emitting state in 5HI. The excitation anisotropy spectrum of 5HI (and 5HW) presented in this work clearly demonstrates that ^1L_b is the emitting state. Also three of the four 5HW proteins investigated show only ^1L_b emission. But 5HW in a protein can also emit from ^1L_a and experimental data collected for W20LysM tandem protein show this for the first time. For this protein dual emission was observed. Because the ^1L_a dipole moment is significantly larger than the ^1L_b dipole moment, inhomogeneous broadening will induce more spectral broadening at the ^1L_a origin. A protein microenvironment increasing this broadening may make ^1L_a the lowest in energy [132], offering an explanation for the dual emission of W20LysM tandem protein.

For the LysM proteins, the emission maxima for the Trp-containing proteins are 341 $\pm$ 1 nm [106], while for the four 5HW LysM proteins the emission maxima appear at 330 - 335 nm (data not shown). Likewise, the emission energies of many other single 5HW containing proteins are blue-shifted compared to their wild type counterpart [133, 100, 134, 78]. Only in a few cases a red-shift was reported [131, 79]. Hirst and coworkers calculated the emission energy of six proteins containing either Trp or 5HW and found the ^1L_a emission energy of 5HW is typically $\approx$ 20 nm (0.2 eV) red-shifted compared to Trp[127]. For 5HW

at a hydrophobic buried position, emission energies for the ^1L_a state of Trp and 5HW were calculated to be quite close to each other. Taken together, the available experimental data of 5HW containing proteins indicates ^1L_b is typically the emitting state, but the protein matrix can promote ^1L_a emission as presented here for the first time for W20LysM tandem protein showing dual emission.

In conclusion, in this work we experimentally show emission of 5HI and free 5HW occurs from the ^1L_b state, a conclusion in line with previous spectroscopic observation typical for ^1L_b emission like a small dependence of λ^{max} on solvent polarity and a high intrinsic anisotropy. Our conclusion is opposite to theoretical calculations predicting ^1L_a as the emitting state for these probes. The protein matrix can make ^1L_a becoming the emitting state, a result not believed to be possible for a long time but now supported theoretically and experimentally. The ability of the protein matrix to tune the emitting state can be exploited as a sensitive probe for monitoring protein conformational changes and probing protein-ligand interactions. Available data however indicate that it might be difficult to meet this condition as most reported 5HW containing proteins show only characteristics corresponding with ^1L_b emission.

Acknowledgments

We thank Dr. P.R. Callis for helpful discussions. This work was supported by the nanotechnology network NanoNed.

4.6 Supplementary figures

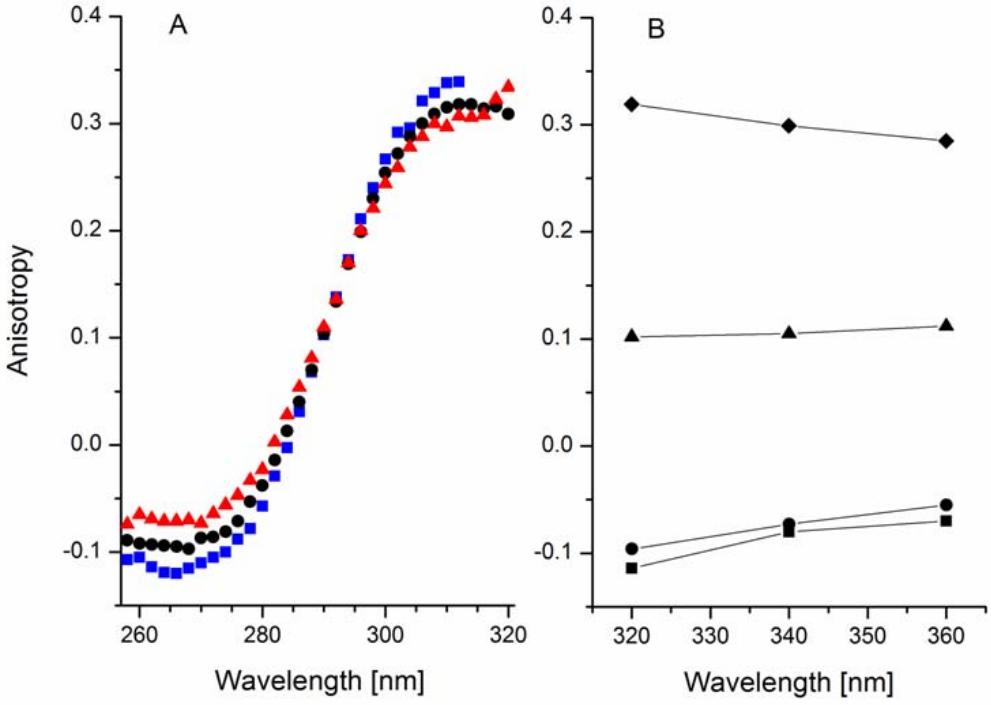

Figure 4.5: Anisotropy excitation spectra of free 5HI in a glycerol glass at -50 °C. Emission was recorded at 320 nm (square), 340 nm (circle) and 360 nm (triangle). **B: Emission wavelength dependence of the anisotropy of free 5HI in a glycerol glass at -50 °C.** Excitation wavelengths of 260 nm (square), 275 nm (circle), 290 nm (triangle), 305 nm (diamond) were used.

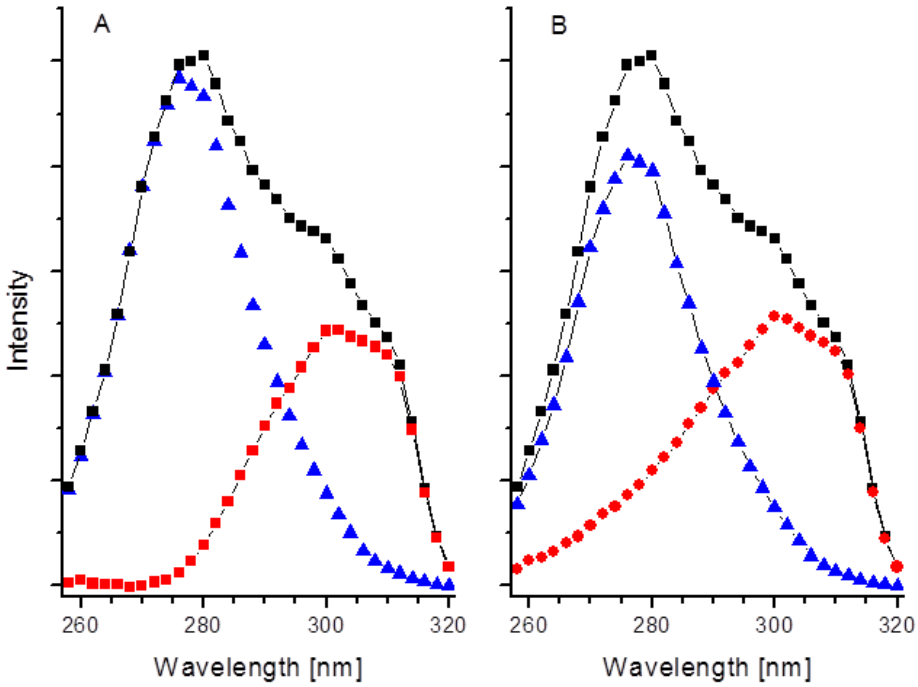

Figure 4.6: Fluorescence excitation spectra (square) of 5HW in a glycerol glass at -50 °C and its resolved ^1L_a (triangle) and ^1L_b (circle) spectra for $\beta = 67°$ (A) and $\beta = 90°$(B).

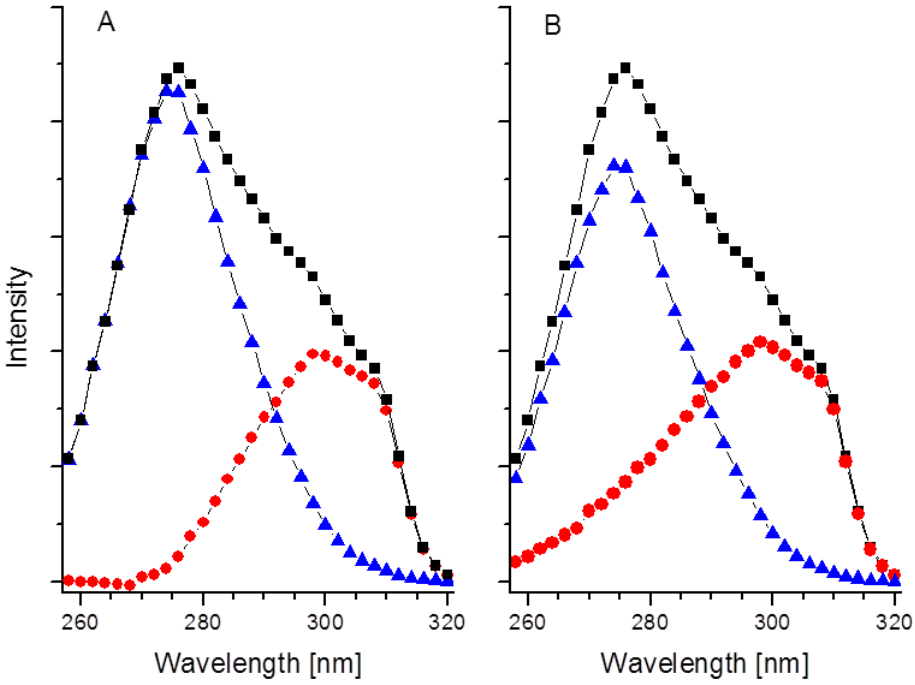

Figure 4.7: Fluorescence excitation spectra (square) of 5HI in a glycerol glass at -50 °C and its resolved ^1L_a (triangle) and ^1L_b (circle) spectra for $\beta = 67°$ (A) and $\beta = 90°$(B).

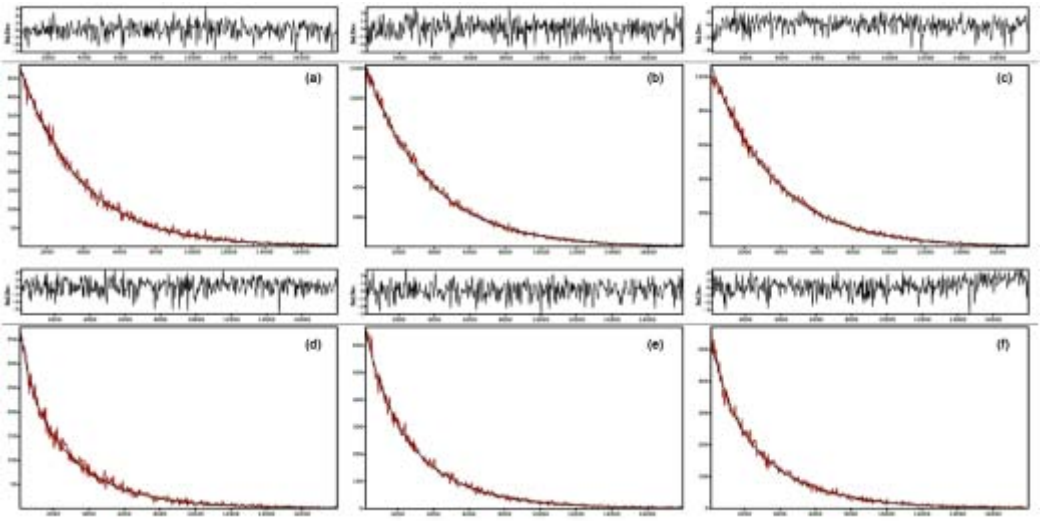

Figure 4.8: Fluorescence decay kinetics of free 5HW at emission wavelengths 320 nm (a), 340 nm (b) and 360 nm (c). **Fluorescence decay kinetics of 5HW containing W20LysM tandem** at emission wavelength 320 nm (d), 340 nm (e) and 360 nm (f).

Chapter 5

Summary

In the last few decades, fluorescence spectroscopy has become a primary research tool in the life sciences and other research fields like medicine and analytical chemistry. In protein chemistry the aromatic amino acid tryptophan (Trp) plays an important role as an intrinsic probe for investigations using this technique. Trp has attractive spectroscopic properties, like a high sensitivity of the spectral energy and quantum yield for a change in microenvironment which allows studying protein structure and dynamics. The high intrinsic anisotropy upon red-edge excitations makes it a valuable probe to investigate site specifically the dynamics in a protein. In practice, these features can only be optimally exploited if purified proteins are used containing only one or two Trp residues.

One approach to overcome this limitation is replacing the Trp of interest by a Trp analogue, which can be biosynthetically incorporated and which shows a red shifted absorbance spectrum, compared to Trp. This allows selective excitation of the analogue in the presence of other tryptophan-containing proteins. These Trp analogue-labelled proteins are also known as spectrally enhanced alloproteins. One of the goals of this PhD work was to explore the use of these proteins as molecular recognition element in a biosensor. The ability to detect microbes this way has been investigated. Moreover, new routes are presented for the production of alloproteins equipped with novel properties that can be exploited in biosensor design and in other research fields.

A concise introduction about Trp fluorescence spectroscopy, incorporation of Trp analogues into recombinant proteins, and LysM domains is given in **chapter 1**.

LysM domains are found in thousands of proteins of prokaryotic and eukaryotic origin. Their affinity for peptidoglycan allows LysM-containing proteins to become non-covalently attached to cell walls and other structures containing this material. A sensitive spectroscopic method allowing the direct monitoring of the binding event has not been reported. In **chapter 2** a fluorescence method is presented to directly measure the interaction of a LysM domain with peptidoglycan. A Trp analogue fluorescence spectroscopy-based method is presented requiring only a few μg of LysM. Four single Trp LysM proteins were constructed and biosynthetically labelled with the Trp analogues 5-hydroxytryptophan (5HW) and 7-azatryptophan. The red-shifted absorption spectra of these analogues allow excitation at wavelengths where tryptophan does not absorb. Thus, samples containing Trp can be analysed with this methodology. This method will help the LysM field in the discovery of new ligands and addressing fundamental research questions like the kinetics of the LysM-ligand interaction. Moreover, the presented single-Trp mutants may find application in a biosensor for the detection of microbes.

To date, a limited number of Trp analogues have been biosynthetically incorporated in proteins, including azaTrps, fluoroTrps, aminoTrps, and hydroxyTrp analogues. In almost all studies, an *E. coli* Trp auxotroph was employed as expression host. The high substrate specificity of the enzyme tryptophan aminoacyl-tRNA synthetase (trpRS) in *E.*

coli limits the incorporation of Trp analogues with bulkier substituents. In **chapter 3** a *Lactococcus lactis* Trp auxotroph expression system is presented able to biosynthetically incorporate in proteins tryptophan analogues with bulky substituents (like chloro- and bromotryptophan and also difluorotryptophan). Alloproteins containing these analogs can now be easily produced in high yields. Coexpression of the trpRS of *Lactococcus lactis* was essential to obtain these results. The developed system features the most relaxed specificity for Trp analogue incorporation reported to date and gives a high alloprotein yield.

Easy access to alloproteins containing chloro- or bromotryptophan offers new opportunities to study structure and dynamics of these proteins using Trp analogue phosphorescence spectroscopy. Chloro- or bromotryptophans are attractive intrinsic phosphorescence probes because they are much less sensitive for quenchers in the medium, like oxygen. The extremely high sensitivity of Trp phosphorescence for quenchers has limited widespread use of this unique spectroscopic method.

A straightforward approach to investigate the involvement of a Trp residue in cation-π or π-π interactions is the characterization of a set of alloproteins, each containing a Trp analogue with a different electron density distribution at the indole moiety. The presented expression system is ideally suited to generate methyl and fluoro-substituted Trp analogue-containing alloproteins for these investigations. To date, these alloproteins are produced in extremely low amounts via an *in vitro* methodology using *Xenopus laevis* oocytes as expression system. This limits analysis of these proteins to very sensitive methodologies like patch-clamp. The availability of these proteins in mg quantities enables studies via other methodologies including fluorescence spectroscopy, NMR, and calorimetry.

The method for the efficient incorporation of Trp analogues, described in **chapter 3**, enabled studying the emitting state of 5HW in proteins and this work is presented in **chapter 4**. A controversy exists in the current literature about the emitting state of 5HW and 5-hydroxyindole (5HI). For a long time it was assumed that these probes were emitting only from the ^1L_b state, although conclusive experimental data, like excitation anisotropy spectra, have not been reported. Recently, two computational studies were published claiming that ^1L_a is the emitting state of 5HI and 5HW when present in polar solvents, including water, and that it is also typically the emitting state of 5HW incorporated in proteins. In **chapter 4** convincing experimental data is presented about the emitting state of 5HI, 5HW, and of 5HW incorporated in 4 proteins. ^1L_b is the emitting state in all these samples except in one protein, which shows dual emission from both the ^1L_a and ^1L_b states.

Given the large differences in the properties of the ^1L_a and ^1L_b states, fluorescent data can only be properly interpreted if the emitting state is known. The data presented in **chapter 4** undermines the long standing consensus view that ^1L_b is the only emitting

state of this popular Trp analogue, as well as the conclusion of the recent papers claiming that ^1L_a is typically the emitting state. The work presented in **chapter 4** settles this issue and a straightforward procedure is presented to estimate the emitting state of these probes. We foresee that this work will become a reference study for future work employing 5-hydroxyindole, 5-hydroxytryptophan, or the neurotransmitter serotonin as fluorescent probes.

Chapter 6

Samenvatting

In de laatste decennia is fluorescentiespectroscopie een belangrijke onderzoeksmethode geworden in de levenswetenschappen en onderzoeksgebieden zoals geneeskunde en analytische chemie. Fluorescentiespectroscopie wordt ook veelvuldig toegepast in eiwitchemisch onderzoek, waarbij het aromatische aminozuur tryptofaan (Trp) vaak wordt gebruikt als fluorescentieprobe. Trp heeft interessante eigenschappen, zoals een hoge gevoeligheid van de emissie-energie en de lichtopbrengst voor een verandering in de microomgeving van Trp. Dit maakt Trp erg geschikt voor het bestuderen van eiwitstructuren en eiwitdynamica. Ook de hoge intrinsieke anisotropie van Trp bij excitatie met golflengtes boven 295 nm biedt goede mogelijkheden om eiwitten te bestuderen, met name met betrekking tot de lokale dynamica van een eiwit. Deze eigenschappen kunnen in de praktijk echter alleen optimaal benut worden, als gezuiverd eiwit met slechts 1 of 2 Trp-residuen gebruikt wordt.

Eén mogelijkheid om een mengsel van eiwitten m.b.v. fluorescentie te bestuderen is het vervangen van een specifieke Trp in één van de eiwitten door een Trp-analogon dat absorbeert bij hogere golflengtes dan Trp zelf. Dit maakt het selectief exciteren van het Trp-analogon mogelijk in aanwezigheid van andere Trp-bevattende eiwitten. Vanwege de aanwezigheid van een onnatuurlijk aminozuur worden deze eiwitten ook wel alloproteïnes genoemd. Eén van de doelen van het promotie project was te onderzoeken of Trp analogon bevattende eiwitten gebruikt kunnen worden als moleculair herkenningselement in een biosensor. Het onderzoek heeft zich voornamelijk toegespitst op de detectie van celwandmateriaal afkomstig van bacteriën. Daarnaast zijn een aantal nieuwe procedures ontwikkeld voor de productie van alloproteïnes met eigenschappen die van belang kunnen zijn voor toepassing in biosensoren en in fundamenteel eiwitchemisch onderzoek.

In **hoofdstuk 1** wordt algemene informatie gegeven over Trp fluorescentiespectroscopie, het inbouwen van Trp-analoga in recombinante eiwitten, en over LysM domeinen. LysM domeinen zijn te vinden in duizenden verschillende eiwitten van prokaryotische en eukaryotische oorsprong. Door hun affiniteit voor peptidoglycan kunnen eiwitten die een LysM domein bevatten binden aan celwanden en aan andere peptidoglycan bevattende stoffen. Tot nu toe was er geen gevoelige spectroscopische methode voorhanden om de interactie tussen LysM domeinen en de celwand direct te kunnen volgen. In **hoofdstuk 2** wordt een fluorescentiemethode gepresenteerd waarmee deze interactie gevolgd kan worden. Voor deze op een Trp-analogon gebaseerde methode is slechts een paar μg LysM nodig per meting. In dit hoofdstuk wordt de productie beschreven van vier verschillende LysM-eiwitten die slechts één Trp bevatten, elk biosynthetisch gelabeld met de Trp-analoga 5-hydroxytryptofaan (5HW) en 7-azatryptofaan. De absorptiespectra van deze analoga vertonen een verschuiving naar hogere golflengte, vergeleken met het absorptiespectrum van Trp. Dit zorgt ervoor dat monsters die ook gewone Trp bevatten via deze methodologie goed geanalyseerd kunnen worden, aangezien geëxciteerd wordt bij

golflengtes van 310-320 nm. De beschreven methode kan het LysM vakgebied helpen bij het ontdekken van nieuwe liganden en het bestuderen van de kinetiek van de LysM-ligand interacties. Daarnaast kunnen de beschreven LysM alloproteïnes een toepassing vinden in biosensoren voor het detecteren van bacteriën.

Tot op heden is er slechts een beperkt aantal Trp-analoga biosynthetisch ingebouwd in eiwitten, zoals bijvoorbeeld aza-, fluoro-, amino- en hydroxytryptofanen. In bijna alle studies werd een Trp auxotrofe *E. coli* stam gebruikt als expressiesysteem. De hoge substraatspecificiteit van het enzym tryptofaan aminoacyl-tRNA synthetase (trpRS) in *E. coli* beperkt het inbouwen van Trp-analoga met grotere substituenten. In **hoofdstuk 3** wordt een *Lactococcus lactis* Trp auxotroof expressie systeem beschreven die de biosynthetische inbouw van Trp analoga met grotere substituenten (zoals chloro- en bromotryptofaan, alsmede difluorotryptofaan) mogelijk maakt. Alloproteïnes die deze analoga bevatten kunnen nu gemakkelijk in hoge opbrengst worden geproduceerd. Co-expressie van trpRS van *Lactococcus lactis* was essentieel om dit mogelijk te maken.

Het op een eenvoudige manier produceren van chloro- of bromotryptofaan bevattende alloproteïnes opent ook nieuwe mogelijkheden om de structuur en dynamica van deze eiwitten te bestuderen met behulp van fosforescentie spectroscopie. Chloro- of bromotryptofanen zijn aantrekkelijke intrinsieke fosforescentie-probes, omdat zij veel minder gevoelig zijn voor quenchers zoals zuurstof. De extreem hoge quencher-gevoeligheid van Trp-fosforescentie heeft toepassing van deze spectroscopische methode in eiwitonderzoek aanzienlijk belemmerd.

Een goede manier om de rol van een Trp-residue in kation-π of π-π interacties te onderzoeken, is het bestuderen van deze interactie in een reeks alloproteïnes die elk een Trp-analogon bevatten met een verschillende electronenverdeling in de indool groep. Het hierboven genoemden expressiesysteem is uitermate geschikt om methyl- en fluorgesubstitueerde Trp bevattende alloproteïnes te produceren. Tot nu toe werden deze alloproteïnes enkel geproduceerd met een zeer lage opbrengst via een in vitro methode die gebruik maakt van *Xenopus laevis* oocyten als expressiesysteem. Dit beperkt de analyse van deze eiwitten tot zeer gevoelige methodes zoals patch-clamp. De nieuwe mogelijkheid om deze eiwitten op mg-schaal te produceren opent de weg voor experimenteel werk via andere analyse methoden zoals fluorescentie, NMR en calorimetrie.

De methode voor de efficiënte inbouw van Trp-analoga, zoals beschreven in **hoofdstuk 3**, maakte het mogelijk om de emissietoestand van 5HW in eiwitten te bestuderen en dit werk is beschreven in **hoofdstuk 4**. De literatuur is niet eenduidig over de emissietoestand van 5HW en 5-hydroxyindool (5HI). Lange tijd werd aangenomen dat deze fluoroforen alleen emissie vertonen vanaf de ^1L_b toestand, maar overtuigend experimenteel bewijs, uit bijvoorbeeld excitatie anisotropie spectra, was niet voorhanden. In twee recente theoretische studies werd geconcludeerd dat ^1L_a de emissietoestand is van 5HI en

5HW in polaire oplosmiddelen, waaronder water, en dat dit ook geldt voor 5HW wanneer deze verbinding is ingebouwd in een eiwit. In **hoofdstuk 4** worden experimentele data gepresenteerd over de emissietoestand van vrij 5HI en 5HW, en van 5HW ingebouwd in een eiwit. Hieruit blijkt dat in de meeste gevallen ^1L_b de emissietoestand is. Echter, één eiwit vertoont zowel ^1L_a en ^1L_b emissie.

5HW fluorescentie data kunnen alleen correct worden geïnterpreteerd als de emissietoestand bekend is. De data in **hoofdstuk 4** ontkrachten de sinds lang geaccepteerde consensus dat ^1L_b de enige emissietoestand is van dit populaire Trp-analogon, en ook de conclusies uit recentere studies die beschrijven dat emissie veelal via ^1L_a plaats vindt. Het onderzoek beschreven in **hoofdstuk 4** lost deze controverse op en draagt een eenvoudige procedure aan om de emissietoestand van deze fluoroforen te bepalen. Dit onderzoek kan een referentiestudie worden voor toekomstige studies die gebruik maken van 5-hydroxyindool, 5-hydroxytryptofaan en de neurotransmitter serotonine als fluorescentieprobes.

Bibliography

[1] G. G. Stokes. On the change of refrangibility of light. *Phil. Trans. R. Soc. London*, 142:463–562, 1852.

[2] A. Jablonski. Über den Mechanisms des Photolumineszenz von Farbstoffphosphoren. *Z. Phys.*, 94:38–46, 1935.

[3] J. R. Lakowicz. *Principles of fluorescence spectroscopy.* Kluwer Academic/Plenum Publishers, New York, 2nd edition edition, 1999.

[4] S. S. Lehrer. Solute perturbation of protein fluorescence. The quenching of the tryptophyl fluorescence of model compounds and of lysozyme by iodide ion. *Biochemistry*, 10(17):3254–3263, 1971.

[5] K. A. Hagaman and M. R. Eftink. Fluorescence quenching of Trp-314 of liver alcohol dehydrogenase by oxygen. *Biophys. Chem.*, 20(3):201–207, 1984.

[6] M. R. Eftink and D. M. Jameson. Acrylamide and oxygen fluorescence quenching studies with liver alcohol dehydrogenase using steady-state and phase fluorometry. *Biochemistry*, 21(18):4443–4449, 1982.

[7] M. R. Eftink and L. A. Selvidge. Fluorescence quenching of liver alcohol dehydrogenase by acrylamide. *Biochemistry*, 21(1):117–125, 1982.

[8] D. Xing, R. Dorr, R. P. Cunningham, and C. P. Scholes. Endonuclease III interactions with DNA substrates. 2. The DNA repair enzyme endonuclease III binds differently to intact DNA and to apyrimidinic/apurinic DNA substrates as shown by tryptophan fluorescence quenching. *Biochemistry*, 34(8):2537–2544, 1995.

[9] A. Robert M. *Lakowicz JR. Fluorescence spectroscopy of biomolecules. In Encyclopedia of Molecular Biology and Molecular Medicine.* . VCH Publisher, New York, 1995.

[10] J. M. Beechem and L. Brand. Time-resolved fluorescence of proteins. *Annu. Rev. Biochem.*, 54:43–71, 1985.

[11] R. Y. Tsien. The green fluorescent protein. *Annu. Rev. Biochem.*, 67(1):509–544, 1998.

[12] A. Fredj, H. Pasquier, I. Demachy, G. Jonasson, B. Levy, V. Derrien, Y. Bousmah, G. Manoussaris, F. Wien, J. Ridard, M. Erard, and F. Merola. The single T65S mutation generates brighter cyan fluorescent proteins with increased photostability and pH insensitivity. *PLoS ONE*, 7(11):e49149, 2012.

[13] R. Heim, A. B. Cubitt, and R. Y. Tsien. Improved green fluorescence. *Nature*, 373(6516):663–664, 1995.

[14] G. Weber. Polarization of the fluorescence of macromolecules. 2. Fluorescent conjugates of ovalbumin and bovine serum albumin. *Biochem. J.*, 51(2):155–167, 1952.

[15] J. Slavik. Anilinonaphthalene sulfonate as a probe of membrane composition and function. *Biochim. Biophys. Acta*, 694(1):1–25, 1982.

[16] M. R. Eftink. Fluorescence techniques for studying protein structure. *Methods Biochem. Anal.*, 35:127–205, 1991.

[17] J. R. Platt. Classification of spectra of cata-condensed hydrocarbons. *J. Chem. Phys.*, 17(5):484–495, 1949.

[18] E. H. Strickland, J. Horwitz, and C. Billups. Near-ultraviolet absorption bands of tryptopan. Studies using indole and 3-methylindole as models. *Biochemistry*, 9(25):4914–4921, 1970.

[19] K. Tveen Jensen, G. Strambini, M. Gonnelli, J. Broos, and J. B. Jackson. Mutations in transhydrogenase change the fluorescence emission state of TRP72 from ^1L_a to ^1L_a. *Biophys. J.*, 95(7):3419–3428, 2008.

[20] J. Broos, K. Tveen-Jensen, E. de Waal, B. H. Hesp, J. B. Jackson, G. W. Canters, and P. R. Callis. The emitting state of tryptophan in proteins with highly blue-shifted fluorescence. *Angew. Chem. Int. Ed.*, 46(27):5137–5139, 2007.

[21] J. T. Vivian and P. R. Callis. Mechanisms of tryptophan fluorescence shifts in proteins. *Biophys. J.*, 80(5):2093–2109, 2001.

[22] J. B. Ross, A. G. Szabo, and C. W. Hogue. Enhancement of protein spectra with tryptophan analogs: fluorescence spectroscopy of protein-protein and protein-nucleic acid interactions. *Meth. Enzymol.*, 278:151–190, 1997.

[23] P. R. Callis and T. Liu. Quantitative prediction of fluorescence quantum yields for tryptophan in proteins. *J. Phys. Chem. B*, 108(14):4248–4259, 2004.

[24] A. B. Pardee, L. S. Prestidge, and V. G. Shore. Incorporation of azatryptophan into proteins of bacteria and bacteriophage. *Biochim. Biophys. Acta*, 21(2):406–407, 1956.

[25] E. W. Davie, V. V. Koningsberger, and F. Lipmann. The isolation of a tryptophan-activating enzyme from pancreas. *Arch. Biochem. Biophys.*, 65(1):21–38, 1956.

[26] N. Sharon and F. Lipmann. Reactivity of analogs with pancreatic tryptophan-activating enzyme. *Arch. Biochem. Biophys.*, 69:219–227, 1957.

[27] S. Schlesinger. The effect of amino acid analogues on alkaline phosphatase. Formation in *Escherichia coli* K-12. II. Replacement of tryptophan by azatryptophan and by tryptazan. *J. Biol. Chem.*, 243(14):3877–3883, 1968.

[28] E. A. Pratt and C. Ho. Incorporation of fluorotryptophans into proteins of *Escherichia coli*. *Biochemistry*, 14(13):3035–3040, 1975.

[29] E. Amann, J. Brosius, and M. Ptashne. Vectors bearing a hybrid trp-lac promoter useful for regulated expression of cloned genes in *Escherichia coli*. *Gene*, 25(2-3):167–178, 1983.

[30] C. W. Hogue, I. Rasquinha, A. G. Szabo, and J. P. MacManus. A new intrinsic fluorescent probe for proteins. Biosynthetic incorporation of 5-hydroxytryptophan into oncomodulin. *FEBS Lett.*, 310(3):269–272, 1992.

[31] J. B. Ross, D. F. Senear, E. Waxman, B. B. Kombo, E. Rusinova, Y. T. Huang, W. R. Laws, and C. A. Hasselbacher. Spectral enhancement of proteins: biological incorporation and fluorescence characterization of 5-hydroxytryptophan in bacteriophage lambda cI repressor. *Proc. Natl. Acad. Sci. USA*, 89(24):12023–12027, 1992.

[32] K. Lotte, R. Plessow, and A. Brockhinke. Static and time-resolved fluorescence investigations of tryptophan analogues-a solvent study. *Photochem. Photobiol. Sci.*, 3(4):348–359, 2004.

[33] Y. Chen, F. Gai, and J. W. Petrich. Single-exponential fluorescence decay of the nonnatural amino acid 7-azatryptophan and the nonexponential fluorescence decay of tryptophan in water. *J. Phys. Chem.*, 98(8):2203–2209, 1994.

[34] L. Kelepouris and G. J. Blanchard. Lifetime and reorientation measurements of 7-azaindole and 7-azatryptophan in aqueous adipic acid solutions: the significance

of pendant functionalities in solution phase association processes. *J. Phys. Chem. A*, 104(31):7261–7267, 2000.

[35] A. C. Borin and L. Serrano-Andrés. A theoretical study of the absorption spectra of indole and its analogs: indene, benzimidazole, and 7-azaindole. *Chem. Phys.*, 262(2-3):253–265, 2000.

[36] J. B. A. Ross, E. Rusinova, L. A. Luck, and K. W. Rousslang. *Spectral enhancement of proteins by in vivo incorporation of tryptophan analogues*, volume 6 of *Topics in Fluorescence Spectroscopy*, pages 17–42. Springer US, 2002.

[37] F. Correa and C. S. Farah. Using 5-hydroxytryptophan as a probe to follow protein-protein interactions and protein folding transitions. *Protein Pept. Lett.*, 12(3):241–244, 2005.

[38] J. Broos, F. Maddalena, and B. H. Hesp. *In vivo* synthesized proteins with mono-exponential fluorescence decay kinetics. *J. Am. Chem. Soc.*, 126(1):22–23, 2004.

[39] G. R. Winkler, S. B. Harkins, J. C. Lee, and H. B. Gray. Alpha-synuclein structures probed by 5-fluorotryptophan fluorescence and ^{19}F NMR spectroscopy. *J. Phys. Chem. B*, 110(13):7058–7061, 2006.

[40] M. Opacic, E. P. Vos, B. H. Hesp, and J. Broos. Localization of the substrate-binding site in the homodimeric mannitol transporter, EIImtl, of *Escherichia coli*. *J. Biol. Chem.*, 285(33):25324–25331, 2010.

[41] P. M. Bronskill and J. T. Wong. Suppression of fluorescence of tryptophan residues in proteins by replacement with 4-fluorotryptophan. *Biochem J.*, 249(1):305–308, 1988.

[42] M. Ibba and D. Soll. Aminoacyl-tRNA synthesis. *Annu. Rev. Biochem.*, 69:617–650, 2000.

[43] F. Chapeville, F. Lipmann, G. von Ehrenstein, B. Weisblum, W. J. Ray Jr, and S. Benzer. On the role of soluble ribonucleic acid in coding for amino acids. *Proc. Natl. Acad. Sci. USA*, 48:1086–1092, 1962.

[44] O. Kotik-Kogan, N. Moor, D. Tworowski, and M. Safro. Structural basis for discrimination of L-phenylalanine from L-tyrosine by phenylalanyl-tRNA synthetase, 2005.

[45] C. J. Noren, S. J. Anthony-Cahill, M. C. Griffith, and P. G. Schultz. A general method for site-specific incorporation of unnatural amino acids into proteins. *Science*, 244(4901):182–188, 1989.

[46] J. Ling, N. Reynolds, and M. Ibba. Aminoacyl-tRNA synthesis and translational quality control. *Annu. Rev. Microbiol.*, 63:61–78, 2009.

[47] D. Datta, P. Wang, I. S. Carrico, S. L. Mayo, and D. A. Tirrell. A designed phenylalanyl-tRNA synthetase variant allows efficient *in vivo* incorporation of aryl ketone functionality into proteins. *J. Am. Chem. Soc.*, 124(20):5652–5653, 2002.

[48] K. L. Kiick, J. C. van Hest, and D. A. Tirrell. Expanding the scope of protein biosynthesis by altering the methionyl-tRNA synthetase activity of a bacterial expression host. *Angew. Chem. Int. Ed.*, 39(12):2148–2152, 2000.

[49] W. Kim, A. George, M. Evans, and V. P. Conticello. Cotranslational incorporation of a structurally diverse series of proline analogues in an *Escherichia coli* expression system. *ChemBioChem*, 5(7):928–936, 2004.

[50] L. Wang, A. Brock, B. Herberich, and P. G. Schultz. Expanding the genetic code of *Escherichia coli*. *Science*, 292(5516):498–500, 2001.

[51] J. C. Anderson, N. Wu, S. W. Santoro, V. Lakshman, D. S. King, and P. G. Schultz. An expanded genetic code with a functional quadruplet codon. *Proc. Natl. Acad. Sci. USA*, 101(20):7566–7571, 2004.

[52] L. Wang and P. G. Schultz. A general approach for the generation of orthogonal tRNAs. *Chem. Biol.*, 8(9):883–890, 2001.

[53] I. Kwon, P. Wang, and D. A. Tirrell. Design of a bacterial host for site-specific incorporation of p-bromophenylalanine into recombinant proteins. *J. Am. Chem. Soc.*, 128(36):11778–11783, 2006.

[54] M. El Khattabi, M. L. van Roosmalen, D. Jager, H. Metselaar, H. Permentier, K. Leenhouts, and J. Broos. *Lactococcus lactis* as expression host for the biosynthetic incorporation of tryptophan analogues into recombinant proteins. *Biochem J.*, 409(1):193–198, 2008.

[55] G. Buist, A. Steen, J. Kok, and O. P. Kuipers. LysM, a widely distributed protein motif for binding to (peptido)glycans. *Mol. Microbiol.*, 68(4):838–847, 2008.

[56] K. J. Garvey, M. S. Saedi, and J. Ito. Nucleotide sequence of *Bacillus* phage phi 29 genes 14 and 15: homology of gene 15 with other phage lysozymes. *Nucleic Acids Res.*, 14(24):10001–10008, 1986.

[57] P. F. Longchamp, C. Mauel, and D. Karamata. Lytic enzymes associated with defective prophages of *Bacillus subtilis*: sequencing and characterization of the region comprising the N-acetylmuramoyl-L-alanine amidase gene of prophage PBSX. *Microbiology*, 140:1855–1867, 1994.

[58] P. Margot, M. Pagni, and D. Karamata. *Bacillus subtilis* 168 gene lytF encodes a gamma-D-glutamate-meso-diaminopimelate muropeptidase expressed by the alternative vegetative sigma factor, sigmaD. *Microbiology*, 145(1):57–65, 1999.

[59] R. Ohnishi, S. Ishikawa, and J. Sekiguchi. Peptidoglycan hydrolase LytF plays a role in cell separation with CwlF during vegetative growth of *Bacillus subtilis*. *J. Bacteriol.*, 181(10):3178–3184, 1999.

[60] A. Steen and G. Buist and K. J. Leenhouts and M. El Khattabi and F. Grijpstra and A. L. Zomer and G. Venema and O. P. Kuipers and J. Kok. Cell wall attachment of a widely distributed peptidoglycan binding domain is hindered by cell wall constituents. *J. Biol. Chem.*, 278(26):23874–23881, 2003.

[61] J. Bielnicki, Y. Devedjiev, U. Derewenda, Z. Dauter, A. Joachimiak, and Z. S. Derewenda. *B. subtilis* ykuD protein at 2.0 A resolution: insights into the structure and function of a novel, ubiquitous family of bacterial enzymes. *Proteins*, 62(1):144–151, 2006.

[62] G. Buist, J. Kok, K. J. Leenhouts, M. Dabrowska, G. Venema, and A. J. Haandrikman. Molecular cloning and nucleotide sequence of the gene encoding the major peptidoglycan hydrolase of *Lactococcus lactis*, a muramidase needed for cell separation. *J. Bacteriol.*, 177(6):1554–1563, 1995.

[63] A. Bateman and M. Bycroft. The structure of a LysM domain from *E. coli* membrane-bound lytic murein transglycosylase D (MltD). *J. Mol. Biol.*, 299(4):1113–1119, 2000.

[64] A. Sasagawa, N. Tochio, K. Saito, S. Koshiba, M. Inoue, T. Kigawa, and S. Yokoyama. The solution structure of the LysM domain of human hypothetical protein SB145. PDB ID: 2DJP.

[65] L. M. Koharudin, A. R. Viscomi, B. Montanini, M. J. Kershaw, N. J. Talbot, S. Ottonello, and A. M. Gronenborn. Structure-function analysis of a CVNH-LysM lectin expressed during plant infection by the rice blast fungus *Magnaporthe oryzae*. *Structure*, 19(5):662–674, 2011.

[66] T. Ohnuma, S. Onaga, K. Murata, T. Taira, and E. Katoh. LysM domains from *Pteris ryukyuensis* chitinase-A: a stability study and characterization of the chitin-binding site. *J. Biol. Chem.*, 283(8):5178–5187, 2008.

[67] M. S. Turner, L. M. Hafner, T. Walsh, and P. M. Giffard. Identification and characterization of the novel LysM domain-containing surface protein Sep from *Lactobacillus fermentum* BR11 and its use as a peptide fusion partner in *Lactobacillus* and *Lactococcus*. *Appl. Environ. Microbiol.*, 70(6):3673–3680, 2004.

[68] G. Buist, H. Karsens, A. Nauta, D. van Sinderen, G. Venema, and J. Kok. Autolysis of *Lactococcus lactis* caused by induced overproduction of its major autolysin, AcmA. *Appl. Environ. Microbiol.*, 63(7):2722–2728, 1997.

[69] A. Steen, G. Buist, G. J. Horsburgh, G. Venema, O. P. Kuipers, S. J. Foster, and J. Kok. AcmA of *Lactococcus lactis* is an N-acetylglucosaminidase with an optimal number of LysM domains for proper functioning. *FEBS J.*, 272(11):2854–2868, 2005.

[70] G. Buist, G. Venema, and J. Kok. Autolysis of *Lactococcus lactis* is influenced by proteolysis. *J. Bacteriol.*, 180(22):5947–5953, 1998.

[71] T. Bosma, R. Kanninga, J. Neef, S. A. Audouy, M. L. van Roosmalen, A. Steen, G. Buist, J. Kok, O. P. Kuipers, G. Robillard, and K. Leenhouts. Novel surface display system for proteins on non-genetically modified gram-positive bacteria. *Appl. Environ. Microbiol.*, 72(1):880–889, 2006.

[72] M. L. van Roosmalen, R. Kanninga, M. El Khattabi, J. Neef, S. Audouy, T. Bosma, A. Kuipers, E. Post, A. Steen, J. Kok, G. Buist, O. P. Kuipers, G. Robillard, and K. Leenhouts. Mucosal vaccine delivery of antigens tightly bound to an adjuvant particle made from food-grade bacteria. *Methods*, 38(2):144–149, 2006.

[73] A. de Haan, B. J. Haijema, P. Voorn, T. Meijerhof, M. L. van Roosmalen, and K. Leenhouts. Bacterium-like particles supplemented with inactivated influenza antigen induce cross-protective influenza-specific antibody responses through intranasal administration. *Vaccine*, 30(32):4884–4891, 2012.

[74] J.B. Ward H.J. Rogers, H.R. Perkins. *The bacterial autolysins. In: Microbial cell walls and membranes*, pages 437–460. Chapman Hall, London, 1980.

[75] B. Joris, S. Englebert, C. P. Chu, R. Kariyama, L. Daneo-Moore, G. D. Shockman, and J. M. Ghuysen. Modular design of the *Enterococcus hirae* muramidase-2 and *Streptococcus faecalis* autolysin. *FEMS Microbiol. Lett.*, 70(3):257–264, 1992.

[76] R. Kariyama and G. D. Shockman. Extracellular and cellular distribution of muramidase-2 and muramidase-1 of *Enterococcus hirae* ATCC 9790. *J. Bacteriol.*, 174(10):3236–3241, 1992.

[77] G. Andre, K. Leenhouts, P. Hols, and Y. F. Dufrêne. Detection and localization of single LysM-peptidoglycan interactions. *J. Bacteriol.*, 190(21):7079–7086, 2008.

[78] Q. Li, H. N. Du, and H. Y. Hu. Study of protein-protein interactions by fluorescence of tryptophan analogs: application to immunoglobulin G binding domain of streptococcal protein G. *Biopolymers*, 72(2):116–122, 2003.

[79] F. Mohammadi, G. A. Prentice, and A. R. Merrill. Protein-protein interaction using tryptophan analogues: novel spectroscopic probes for toxin-elongation factor-2 interactions. *Biochemistry*, 40(34):10273–10283, 2001.

[80] P. E. Kolenbrander and J. C. Ensign. Isolation and chemical structure of the peptidoglycan of *Spirillum serpens* cell walls. *J. Bacteriol.*, 95(1):201–210, 1968.

[81] M. P. Chapot-Chartier, E. Vinogradov, I. Sadovskaya, G. Andre, M. Y. Mistou, P. Trieu-Cuot, S. Furlan, E. Bidnenko, P. Courtin, C. Pechoux, P. Hols, Y. F. Dufrene, and S. Kulakauskas. Cell surface of *Lactococcus lactis* is covered by a protective polysaccharide pellicle. *J. Biol. Chem.*, 285(14):10464–10471, 2010.

[82] R. Wheeler, S. Mesnage, I. G. Boneca, J. K. Hobbs, and S. J. Foster. Super-resolution microscopy reveals cell wall dynamics and peptidoglycan architecture in ovococcal bacteria. *Mol. Microbiol.*, 82(5):1096–1109, 2011.

[83] J. Sambrook, E. F. Fritsch, T. Maniatis, and N. Ford. *Molecular cloning : a laboratory manual*. Cold Spring Harbor Laboratory Press, Cold Spring Harbor, N.Y., 2 edition, 1989.

[84] O. P. Kuipers, P. G. de Ruyter, M. Kleerebezem, and W. M. de Vos. Controlled overproduction of proteins by lactic acid bacteria. *Trends. Biotechnol.*, 15(4):135–140, 1997.

[85] H. Holo and I. F. Nes. Transformation of *Lactococcus* by electroporation. *Methods Mol. Biol.*, 47:195–199, 1995.

[86] B. E. Terzaghi and W. E. Sandine. Improved medium for lactic streptococci and their bacteriophages. *Appl. Microbiol.*, 29(6):807–813, 1975.

[87] B. Poolman and W. N. Konings. Relation of growth of *Streptococcus lactis* and *Streptococcus cremoris* to amino acid transport. *J. Bacteriol.*, 170(2):700–707, 1988.

[88] G. Vriend. WHAT IF: a molecular modeling and drug design program. *J. Mol. Graph.*, 8(1):52–6, 29, 1990.

[89] G. M. Morris, D. S. Goodsell, R. S. Halliday, R. Huey, W. E. Hart, R. K. Belew, and A. J. Olson. Automated docking using a Lamarckian genetic algorithm and an empirical binding free energy function. *J. Comp. Chem.*, 19(14):1639–1662, 1998.

[90] C. Huard, G. Miranda, Y. Redko, F. Wessner, S. J. Foster, and M. P. Chapot-Chartier. Analysis of the peptidoglycan hydrolase complement of *Lactococcus lactis*: identification of a third N-acetylglucosaminidase, AcmC. *Appl. Environ. Microbiol.*, 70(6):3493–3499, 2004.

[91] C. Hetenyi and D. van der Spoel. Efficient docking of peptides to proteins without prior knowledge of the binding site. *Protein Sci.*, 11(7):1729–1737, 2002.

[92] D. Neumann, O. Kohlbacher, H. P. Lenhof, and C. M. Lehr. Lectin-sugar interaction. Calculated versus experimental binding energies. *Eur. J. Biochem.*, 269(5):1518–1524, 2002.

[93] G. M. Morris, D. S. Goodsell, R. Huey, and A. J. Olson. Distributed automated docking of flexible ligands to proteins: parallel applications of AutoDock 2.4. *J. Comput.-Aided Mol. Des.*, 10(4):293–304, 1996.

[94] D. S. Goodsell, G. M. Morris, and A. J. Olson. Automated docking of flexible ligands: applications of AutoDock. *J. Mol. Recognit.*, 9(1):1–5, 1996.

[95] J. Broos, F. ter Veld, and G. T. Robillard. Membrane protein-ligand interactions in *Escherichia coli* vesicles and living cells monitored via a biosynthetically incorporated tryptophan analogue. *Biochemistry*, 38(31):9798–9803, 1999.

[96] W. A. Hendrickson, J. R. Horton, and D. M. LeMaster. Selenomethionyl proteins produced for analysis by multiwavelength anomalous diffraction (MAD): a vehicle for direct determination of three-dimensional structure. *EMBO J.*, 9(5):1665–1672, 1990.

[97] J. T. Wong. Membership mutation of the genetic code: loss of fitness by tryptophan. *Proc. Natl. Acad. Sci. USA*, 80(20):6303–6306, 1983.

[98] N. Budisa, C. Minks, S. Alefelder, W. Wenger, F. Dong, L. Moroder, and R. Huber. Toward the experimental codon reassignment in vivo: protein building with an expanded amino acid repertoire. *FASEB J.*, 13(1):41–51, 1999.

[99] J. C. van Hest and D. A. Tirrell. Efficient introduction of alkene functionality into proteins *in vivo*. *FEBS Lett.*, 428(1-2):68–70, 1998.

[100] C. Y. Wong and M. R. Eftink. Biosynthetic incorporation of tryptophan analogues into staphylococcal nuclease: effect of 5-hydroxytryptophan and 7-azatryptophan on structure and stability. *Protein Sci.*, 6(3):689–697, 1997.

[101] J. Broos, E. Gabellieri, E. Biemans-Oldehinkel, and G. B. Strambini. Efficient biosynthetic incorporation of tryptophan and indole analogs in an integral membrane protein. *Protein Sci.*, 12(9):1991–2000, 2003.

[102] S. Lepthien, B. Wiltschi, B. Bolic, and N. Budisa. *In vivo* engineering of proteins with nitrogen-containing tryptophan analogs. *Appl. Microbiol. Biotechnol.*, 73(4):740–754, 2006.

[103] N. Budisa. Prolegomena to future experimental efforts on genetic code engineering by expanding its amino acid repertoire. *Angew. Chem. Int. Ed.*, 43(47):6426–6463, 2004.

[104] I. Kwon and D. A. Tirrell. Site-specific incorporation of tryptophan analogues into recombinant proteins in bacterial cells. *J. Am. Chem. Soc.*, 129(34):10431–10437, 2007.

[105] M. van de Guchte, J. M. van der Vossen, J. Kok, and G. Venema. Construction of a lactococcal expression vector: expression of hen egg white lysozyme in *Lactococcus lactis* subsp. lactis. *Appl. Environ. Microbiol.*, 55(1):224–228, 1989.

[106] D. M. Petrović, K. Leenhouts, M. L. van Roosmalen, F. Kleinjan, and J. Broos. Monitoring lysin motif-ligand interactions via tryptophan analog fluorescence spectroscopy. *Anal. Biochem.*, 428(2):111–118, 2012.

[107] G. Blaser, M. J. Sanderson, S. A. Batsanov, and A. K. J. Howard. The facile synthesis of a series of tryptophan derivatives. *Tetrahedron Lett.*, 49(17):2795–2798, 2008.

[108] L. L. Melhado and N. J. Leonard. An efficient synthesis of azidoindoles and azidotryptophans. *J. Org. Chem.*, 48(25):5130–5133, 1983.

[109] U. Wegmann, M. O'Connell-Motherway, A. Zomer, G. Buist, C. Shearman, C. Canchaya, M. Ventura, A. Goesmann, M. J. Gasson, O. P. Kuipers, D. van Sinderen, and J. Kok. Complete genome sequence of the prototype lactic acid bacterium *Lactococcus lactis* subsp. cremoris MG1363. *J. Bacteriol.*, 189(8):3256–3270, 2007.

[110] J. M. van der Vossen, D. van der Lelie, and G. Venema. Isolation and characterization of *Streptococcus cremoris* Wg2-specific promoters. *Appl. Environ. Microbiol.*, 53(10):2452–2457, 1987.

[111] O. P. Kuipers, P. G. G. A. de Ruyter, M. Kleerebezem, and W. M. de Vos. Quorum sensing-controlled gene expression in lactic acid bacteria. *J. Biotech.*, 64(1):15–21, 1998.

[112] W. Zhong, J. P. Gallivan, Y. Zhang, L. Li, H. A. Lester, and D. A. Dougherty. From ab initio quantum mechanics to molecular neurobiology: A cation-π binding site in the nicotinic receptor. *Proc. Natl. Acad. Sci. USA*, 95(21):12088–12093, 1998.

[113] J. M. Vanderkooi, D. B. Calhoun, and S. W. Englander. On the prevalence of room-temperature protein phosphorescence. *Science*, 236(4801):568–569, 1987.

[114] G. Veldhuis, E. Gabellieri, E. P. P. Vos, B. Poolman, G. B. Strambini, and J. Broos. Substrate-induced conformational changes in the membrane-embedded IICmtl-domain of the mannitol permease from *Escherichia coli*, enzymeIImtl, probed by tryptophan phosphorescence spectroscopy. *J. Biol. Chem.*, 280(42):35148–35156, 2005.

[115] G. B. Strambini, B. A. Kerwin, B. D. Mason, and M. Gonnelli. The triplet-state lifetime of indole derivatives in aqueous solution. *Photochem. Photobiol.*, 80(3):462–470, 2004.

[116] J. G. Milton, R. M. Purkey, and W. C. Galley. The kinetics of solvent reorientation in hydroxylated solvents from the exciting-wavelength dependence of chromophore emission spectra. *J. Chem. Phys.*, 68(12):5396–5404, 1978.

[117] X. Shen and J. R. Knutson. Subpicosecond fluorescence spectra of tryptophan in water. *J. Phys. Chem. B*, 105(26):6260–6265, 2001.

[118] B. Valeur and G. Weber. Resolution of the fluorescence excitation spectrum of indole into the ^1L_a and ^1L_b excitation bands. *Photochem. Photobiol.*, 25(5):441–444, 1977.

[119] P. R. Callis. ^1L_a and ^1L_b transitions of tryptophan: applications of theory and experimental observations to fluorescence of proteins. *Meth. Enzymol.*, 278:113–150, 1997.

[120] D. W. Pierce and S. G. Boxer. Stark effect spectroscopy of tryptophan. *Biophys. J.*, 68(4):1583–1591, 1995.

[121] T. Kishi, M. Tanaka, and J. Tanaka. Electronic absorption and fluorescence spectra of 5-Hydroxytryptamine (serotonin). Protonation in the excited state. *Bull. Chem. Soc. Jpn.*, 50(5):1267–1271, 1977.

[122] H. Lami. On the possible role of a mixed valence-Rydberg state in the fluorescence of indoles. *J. Phys. Chem.*, 67(7):3274–3281, 1977.

[123] J. Catalán, P. Perez, and A. U. Acuña. Indole spectroscopy: The location of the ^1L_a and ^1L_b electronic states and the absorption spectrum. *J. Mol. Struct.*, 142:179, 1986.

[124] B. Sengupta, J. Guharay, and P. K. Sengupta. 5-Hydroxyindole: usefulness as a novel optical probe. *J. Mol. Struct.*, 559(1-3):347, 2001.

[125] B. Sengupta, J. Guharay, and P. K. Sengupta. Luminescence behaviour of 5-hydroxyindole in different environments. *Spectrochim. Acta, Part A*, 56(6):1213–1221, 2000.

[126] D. Robinson, N. A. Besley, E. A. Lunt, P. O'Shea, and J. D. Hirst. Electronic structure of 5-hydroxyindole: from gas phase to explicit solvation. *J. Phys. Chem.B*, 113(8):2535–2541, 2009.

[127] D. Robinson, N. A. Besley, P. O'Shea, and J. D. Hirst. Calculating the fluorescence of 5-hydroxytryptophan in proteins. *J. Phys. Chem. B*, 113(43):14521–14528, 2009.

[128] D. M. Petrović, K. Leenhouts, M. L. van Roosmalen, and J. Broos. An expression system for the efficient incorporation of an expanded set of tryptophan analogues. *Amino acids*, 44(5):1329–1336, 2013.

[129] W. H. Press, S. A. Teukolsky, W. T. Vetterling, and B. P. Flannery. *Numerical Recipes 3rd Edition: The Art of Scientific Computing*. Cambridge University Press, New York, NY, USA, 3 edition, 2007.

[130] M. R. Eftink, L. A. Selvidge, P. R. Callis, and A. A. Rehms. Photophysics of indole derivatives: experimental resolution of L_a and L_b transitions and comparison with theory. *J. Phys. Chem.*, 94(9):3469–3479, 1990.

[131] C. Y. Wong and M. R. Eftink. Incorporation of tryptophan analogues into staphylococcal nuclease, its V66W mutant, and Delta 137-149 fragment: spectroscopic studies. *Biochemistry*, 37(25):8938–8946, 1998.

[132] T. Liu, P. R. Callis, B. H. Hesp, M. de Groot, W. J. Buma, and J. Broos. Ionization potentials of fluoroindoles and the origin of nonexponential tryptophan fluorescence decay in proteins. *J. Am. Chem. Soc.*, 127(11):4104–4113, 2005.

[133] W. R. Laws, G. P. Schwartz, E. Rusinova, G. T. Burke, Y. Chu, P. G. Katsoyannis, and J. B. A. Ross. 5-Hydroxytryptophan: An absorption and fluorescence probe which is a conservative replacement for [A14 tyrosine] in insulin. *J. Protein. Chem.*, 14(4):225–232, 1995.

[134] K. Das, K. D. Ashby, A. V. Smirnov, F. C. Reinach, J. W. Petrich, and C. S. Farah. Fluorescence properties of recombinant tropomyosin containing tryptophan, 5-hydroxytryptophan and 7-azatryptophan. *Photochem. Photobiol.*, 70(5):719–730, 1999.

Acknowledgments

It was the 17^{th} of November 2006, on my 24^{th} birthday, and just another ordinary day for me as a researcher in the laboratory of Enzymology at the Faculty of Chemistry in Belgrade. That afternoon a colleague entered the laboratory and asked: "Anyone interested in applying for a PhD position in protein biochemistry in Groningen, the Netherlands?", "Why not?" I replied. He gave me the contact details of a person with whom I should discuss the position, and from that moment onwards my 7 years long journey started.

At these very last pages of my thesis I wish to mention and acknowledge people who were directly or indirectly involved in this whole journey.

I would like to thank my promotor Professor Bauke Dijkstra for his support during my PhD training. His help and scientific advices were especially useful for finalizing my thesis manuscript at the end of my PhD period. Thank you Bauke for everything, thank you for always being in the right place at the right time.

I am thankful to my supervisor Dr. Jaap Broos for giving me the opportunity to become a part of the fluorescence world. Jaap thank you for your guidance, big help during the writing period and also valuable life experience. I really appreciate all the freedom you gave me during my research.

To my current boss Professor Katja Loos, thank you for your understanding, trust and friendliness in every possible way. You are a source of positive energy that inspires.

I am grateful to all the people from BioMaDe Technology Foundation, especially Dr. Kees Leenhouts and Dr. Maarten van Roosmalen who made the start of my PhD project smooth, interesting and fun. Thank you, Maarten for being a great daily supervisor. Saška and Kees, you are both wonderful people, BIG thanks to you for everything.

I am grateful to the members of my thesis reading committee, Professor Egbert Boekema, Professor George Robillard and Professor Jan Kok, for the time and effort they have put in improving my manuscript.

I would also like to thank my colleagues from the Protein crystallography group for the great times we have spent together. Hilda you are a fantastic secretary and person. I will never forget the picnics with Henk and you. Andy, Anke, Tjaard and Henriëtte, thank you for always having more than useful comments and suggestions during our group meetings and (for me often difficult) trial talks. Kor and Johan, thank you for being there for many problems and issues. To all my friends and colleagues who made the day-to-day work in the lab more interesting and fun: Marcel, Niels, Ali, Eswar, Hendrike, Renske, Emilie, Francesca, Jelle, Roman, Gjalt, Guntur, Pramod, thank you all for great moments we had in and out of the lab.

I would also like to acknowledge my collaborator Ben Hesp from the Optical Physics of Condensed Matter group, thank you for all the help you gave me with handling of the laser.

My current working environment would not be so nice and pleasant without Erythrina,

Vincent, Anton, Jakob, Kamlesh, Zheng, Salomeh, Albert, Martijn, Jin, Yi, Agnieszka, JanWillem, Guiseppe, Alessio and Diego. Thank you!

During my PhD journey I did not only expand my scientific views, but I also have learned a lot about the world around me and myself. Many friendships and contacts that I made in Groningen have influenced me to become what I am today. Therefore, this acknowledgment would not be complete without mentioning a few more names. Thank you my Balkan and my Hippie community (in no special order): Katarina&Vibor, Višnja&Goran, Ivana&Ivan, Jelena&Slobodan, Jelena&Duško, Milica Spasojević, Milica Stanković, Jelena Stevanović, Igor Kalinić, Katarina Polajnar Horvat, Matilda, Danijela, Nemanja, Katica, Andrija, Bore, Jana; families Popov-Čeleketić, Šaplaić, Ćurčić-Blake, Vujičić-Žagar. My all around the world friends and pals: Gaston, Ana, Tita, Aysa, Elizabeth, Dimitry, Anatol, Wouter, Filippo, Alessio, Simon, Janja, Cécil, Anca, Alok, Laura. Thank you for the unique Groningen experience.

Special thanks to Ralph not only for translating the summary into Dutch, but also for numerous pool games and beers we had.

My dear paranymphs, I shared with you most of my battles and you did an excellent job in being great support all this years. Miki, you "brought" me here, and I never regretted the decision I made. Cimeru-Primzi, thank you for deep friendship, fantastic cuisine (and memorable dinners), and all our "consultations". With all my heart I wish you all the best in life, you both deserve that.

I often used to say that I feel like I have been living two parallel lives - one life "here" in the Netherlands and another one "there" in Serbia (and Bosnia). During all these years my family and friends from Serbia and Bosnia were the endless fountain of support.

Milena&Darko, Jelena&Tome, Milica&Mladen and Kum Marko, thank you for the great times we always shared (and will share) during my short holiday visits.

Draga tetka Stanka, tetak Milan, Jelena i Vule, od srca vam hvala na ljubavi i pažnji, i svim našim zajedničkim, toplim i iskrenim momentima koji zauzimaju posebno mesto u mom životu.

Dragi moji, mama i tata, HVALA VAM na bezgraničnoj ljubavi i podršci koju mi pružate za sve moje životne odluke. Bez vaše podrške sve ovo bi bilo mnogo teže i drugačije.

Ljubo moja, you came to my life just before the end of this journey. I am happy and grateful to have you here, as a cherry on top of the cake, and my true love. Together with you this journey gets a real happy end!

Dejan Petrović
Groningen, February 2014

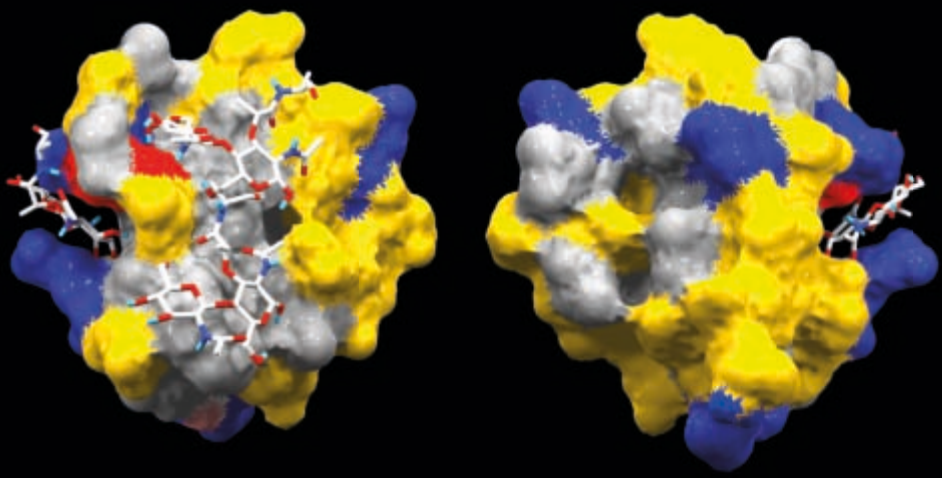

ISBN: 978-90-367-6737-8
ISBN: 978-90-367-6736-1 (electronic version)